Digital Financial Infrastructure and Climate Resilience: Evidence from Mobile Money Adoption

Minjie Guo Stephen A. Karolyi

Uchenna C. Onuoha Leili Pour Rostami

March 2026

Abstract

Does digital finance help communities withstand drought? We study 132 cities across 34 fragile and conflict-affected states over 2000–2021 using satellite vegetation data. A one-standard-deviation soil moisture deficit reduces vegetation by 3.8%, controlling for lagged drought to account for natural vegetation rebound. Mobile money nearly fully offsets this loss: the drought×mobile-money coefficient is +0.035 ($p < 0.05$), stable across progressive controls. In an encompassing specification, mobile money survives while bank branches and credit do not. Event study difference-in-differences estimates confirm that mobile money raises GDP while displacing formal credit, suggesting a transfers-and-savings channel rather than credit intermediation.

JEL Codes: G21, G23, O16, Q54, O33
Keywords: Mobile money, climate adaptation, drought, fintech, financial inclusion, NDVI, Africa

[0]Minjie Guo is at Zhejiang University of Finance and Economics. E-mail: mia_guo667@zufe.edu.cn. Stephen Karolyi is at George Mason University, Costello College of Business. E-mail: skarolyi@gmu.edu. Uchenna C. Onuoha is at the University of Massachusetts Boston, Finance Department. E-mail: uchenna.onuoha001@umb.edu. Leili Pour Rostami is at the University of Massachusetts Boston, Finance Department. E-mail: leili.pourrostami@umb.edu. We thank seminar participants at George Mason University and the University of Massachusetts Boston for helpful comments. All errors are our own.

Disclosure Statement

The authors declare that they have no financial relationships, personal relationships, or other potential conflicts of interest that could have influenced the research, analysis, or conclusions presented in this paper.

1 Introduction

When drought strikes the Sahel, it destroys more than crops. It forces a sequence of economic decisions (whether to sell livestock at distressed prices, withdraw children from school, or attempt seasonal migration) that depends critically on access to savings, credit, and the ability to receive transfers from relatives in less-affected areas. The difference between a community that recovers within a single growing season and one that enters a persistent poverty trap often comes down to finance (Dercon, 2004; Hallegatte et al., 2017). Yet the financial systems of the countries most exposed to climate risk remain among the shallowest in the world: the median country in our sample has fewer than five bank branches per 100,000 adults and domestic credit below 15 percent of GDP.

The rapid spread of mobile money across Sub-Saharan Africa since 2007, reaching over 500 million registered accounts by 2020 (GSMA, 2021), represents a first-order structural change in financial access for populations previously excluded from formal intermediation. Mobile money allows users to store value, send and receive transfers, and make payments using a basic mobile phone without requiring a bank account. The technology is particularly transformative in rural areas where the nearest bank branch may be a day's journey away but mobile network coverage is nearly ubiquitous. Whether this technological transformation matters for climate adaptation is a question with large policy stakes and, until now, little causal evidence.

This paper asks whether mobile money causally affects the capacity of communities in frontier markets to recover from drought, and whether digital financial infrastructure dominates traditional banking in providing this resilience. The questions sit at the intersection of three active literatures that have developed largely in isolation.

Climate economics has established that temperature and precipitation shocks reduce economic output in poor countries, with effects that can persist for years (Dell, Jones, and Olken, 2012; Burke, Hsiang, and Miguel, 2015; Dell, Jones, and Olken, 2014), but has identified few specific, policy-manipulable moderators of these damages (Carleton and Hsiang, 2016). The

available evidence overwhelmingly documents damages; it says much less about what helps.

Financial development research has demonstrated that credit access matters for growth and resilience to macroeconomic shocks (King and Levine, 1993; Levine, 2005; Rajan and Zingales, 1998; McDermott, Barry, and Tol, 2014), but has focused on the *level* of financial development (more credit, more branches) without asking whether the *form* of intermediation matters. A country with 50 percent credit-to-GDP and one with widespread mobile money may look similar on a financial development index, but the distributional and functional properties of their financial systems differ fundamentally.

The digital finance literature has documented transformative effects of mobile money on consumption smoothing and poverty reduction at the household level (Jack and Suri, 2014; Suri and Jack, 2016; Riley, 2018), but has not examined whether these micro-level benefits aggregate to community-level climate resilience or how they compare to the effects of traditional banking. Our contribution is to show that the form of financial infrastructure matters: mobile money nearly fully attenuates drought damage to vegetation while bank branch density does not, and mobile money adoption displaces rather than complements formal credit, suggesting that digital and traditional financial intermediation operate through fundamentally different channels.

We study a panel of 132 cities across 34 fragile and conflict-affected states from 2000 to 2021, yielding 2,776 city-year observations (2,644 in panel regressions that include a one-year lag of drought). Our primary outcome is a satellite-derived vegetation index: the share of farmland pixels above the NDVI vegetation threshold, log-transformed as $\ln(1 + \text{veg share})$. NDVI has been extensively validated as a proxy for agricultural production in agrarian economies (Lobell, Schlenker, and Costa-Roberts, 2011; Burke and Lobell, 2017; Donaldson and Storeygard, 2016), and in our sample, within-country NDVI changes are positively correlated with GDP growth ($\hat{\beta} = 0.480$, $p < 0.001$ in panel regressions with country fixed effects). We measure drought using continuous soil moisture deficit anomalies from the MERRA-2 reanalysis, standardized to each city's own climatological baseline so that a value

of one represents a one-standard-deviation departure from normal conditions.

Our lead specification is a static panel regression of log vegetation on continuous drought severity interacted with mobile money availability, with city and year fixed effects, the mobile money main effect, a one-year lag of drought severity to control for natural vegetation rebound dynamics, and controls for heat stress, rainfall deficit, conflict, and radiation. The drought×mobile-money coefficient is +0.035 ($p < 0.05$), stable across five progressive control specifications that sequentially add these controls. The coefficient ranges from +0.032 to +0.035 on 2,644 observations (the full sample less one year lost to the lag), implying that mobile money nearly fully offsets a one-standard-deviation drought. Adding controls shifts the estimate by less than 10 percent, suggesting minimal observable confounding. Alternative climate shock measures (weighted stress indices, persistent drought, binary onset, compound drought-rain interactions) yield positive attenuation coefficients in all five cases, with four of five reaching at least marginal significance.

We use city-level vegetation indices as our primary outcome because they provide direct, high-frequency measurement of the physical impact channel while preserving the within-country granularity needed for identification. Testing drought×mobile-money attenuation on four outcomes (city-level NDVI, GDP per capita, agricultural value added, and cereal yield) reveals that city-level NDVI is the only outcome with sufficient statistical power to detect attenuation ($t = 2.12$). Country-level aggregates show directionally consistent but imprecise estimates ($|t| < 1.9$), as expected given the nearly fourfold reduction in sample size from 2,644 city-year to approximately 700 country-year observations. NDVI captures the immediate biological impact of drought before markets, policy, and trade filter the signal into downstream aggregates.

A cross-hazard placebo test provides further support for the drought-specific financial channel. The drought-by-mobile-money interaction is significant (+0.035, $p < 0.05$) while the heat-by-mobile-money interaction is insignificant (+0.007), ruling out the concern that mobile money merely proxies for general institutional quality. The sharpest finance result

comes from an encompassing specification that simultaneously includes mobile money, bank branch density, and private credit interacted with drought. Mobile money is the only significant moderator ($+0.039$, $p < 0.05$) while neither bank branches nor credit is significant. This result is specifically about digital financial infrastructure outperforming traditional banking as a buffer against climate shocks.

We complement the panel analysis with two-stage difference-in-differences event studies of mobile money adoption itself, following the approach in Gardner (2022). Joint Wald tests for pre-period coefficients fail to reject the null of parallel trends across all outcomes (p-values: 0.546 for GDP, 0.946 for agricultural value added, 0.735 for credit). Post-adoption, GDP per capita rises by approximately 11 percent within five years ($p < 0.05$), agricultural value added as a share of GDP declines by 3.9 percentage points ($p < 0.05$), and domestic credit falls by 2.1 percentage points. GDP rising while credit *falls* implies that mobile money operates through transfers and savings rather than credit intermediation, challenging the assumption that expanding formal credit is the primary pathway through which finance promotes resilience (King and Levine, 1993; Rajan and Zingales, 1998).

Our work is most closely related to three papers. Burgess et al. show that India's rural bank branch expansion reduced the mortality impact of extreme heat by roughly a factor of ten, demonstrating that financial infrastructure matters for climate resilience, but studying the traditional, physical form. Bharadwaj, Jack, and Suri (2021) show that fintech loans improve household resilience in Kenya, providing micro-level evidence for digital finance. And Jack and Suri (2014) demonstrate that M-Pesa users in Kenya smooth consumption during negative income shocks. We advance this literature in three ways. First, we provide the first multi-country, community-level evidence linking digital financial infrastructure to climate resilience. Second, we directly compare digital and traditional financial infrastructure in the same specification and find that digital dominates. Third, we show that mobile money displaces formal credit while improving welfare, identifying the channel as transfers and savings rather than credit intermediation.

The remainder of the paper is organized as follows. Section 2 describes the data and measurement. Section 3 presents the empirical strategy. Section 4 reports results. Section 5 discusses robustness. Section 6 concludes.

2 Data and Measurement

We assemble a city-year panel of 132 cities across 34 fragile and conflict-affected states, observed annually from 2000 to 2021 (2,776 city-year observations; 2,644 in panel regressions that include a one-year lag of drought). The sample spans Sub-Saharan Africa (22 countries, 81 cities), the Middle East, South and Central Asia, Southeast Asia, and other regions (12 countries, 51 cities). The panel merges satellite-derived vegetation and climate data with country-level indicators of mobile money adoption, financial development, institutional characteristics, and conflict. This section describes each data source; the Internet Appendix provides additional detail on variable construction, the satellite image processing pipeline, and city-by-city visualizations of the delineated farmland areas.

2.1 Vegetation Index (NDVI)

Our primary outcome variable is the Normalized Difference Vegetation Index (NDVI) derived from the Landsat satellite constellation (Landsat 5 TM, 7 ETM+, 8 OLI, and 9). NDVI is defined as the ratio of the difference between near-infrared (NIR) and visible red reflectance to their sum:

$$\text{NDVI} = \frac{\text{NIR} - \text{Red}}{\text{NIR} + \text{Red}} \tag{1}$$

NDVI ranges from -1 to $+1$, with values between 0.2 and 0.8 corresponding to vegetated surfaces. Higher values indicate denser and healthier vegetation.

For each city in the sample, we obtain high-resolution satellite imagery from EarthExplorer, provided by the United States Geological Survey. The construction of the vegetation measure proceeds in four steps. First, for each city, we manually delineate the boundaries

of farmland and agricultural areas within the urban and peri-urban footprint, effectively excluding areas of natural (non-agricultural) vegetation, water bodies, and built-up areas. Figure A.1 in the Internet Appendix illustrates an example of the delineated farmland boundaries. Second, we extract the spectral bands needed for NDVI computation, specifically the near-infrared (Band 5) and visible red (Band 4) rasters, from the clipped satellite imagery. Third, we compute pixel-level NDVI values using equation (1). Fourth, we aggregate the pixel-level NDVI values into a city-year vegetation share by computing the fraction of farmland pixels with NDVI above 0.2, the standard vegetation threshold. This share, denoted veg_{it}, is bounded between zero and one and has a sample mean of approximately 0.52, with higher values indicating that a larger proportion of a city's farmland is vegetated. Appendix Figure A.2 illustrates this workflow using Kosovo as an example. The Internet Appendix provides the delineated farmland boundaries for each of the 132 cities in the sample.

We use the winter (dry season) NDVI composite for each city, which captures permanent vegetation cover and irrigated agriculture while minimizing cloud contamination that plagues wet-season imagery. Our main outcome variable is $\ln(1+\text{veg}_{it})$. The $\ln(1+\cdot)$ transformation accommodates zeros, normalizes the distribution, and renders coefficients interpretable as approximate percent changes in vegetation share.

NDVI has been extensively validated as a proxy for agricultural production and economic activity in developing countries. Burke and Lobell (2017) demonstrate that NDVI predicts crop yields and output variation in smallholder African farming systems with high fidelity. Henderson, Storeygard, and Weil (2012) show that satellite-derived measures can substitute for unreliable national accounts data, and Donaldson and Storeygard (2016) survey the growing use of remotely sensed data in economics. In our sample, within-country changes in log vegetation share are positively correlated with GDP growth ($\hat{\beta} = 0.480$, $p < 0.001$ in panel regressions with country fixed effects), consistent with agriculture constituting 30–60 percent of GDP in most sample countries.

2.2 Climate Variables

Climate data come from NASA's Modern-Era Retrospective Analysis for Research and Applications, Version 2 (MERRA-2; Gelaro et al., 2017). MERRA-2 is a global atmospheric reanalysis that assimilates satellite observations and ground-station data to produce spatially and temporally continuous fields at 0.5° latitude × 0.625° longitude resolution (≈50 km) with hourly temporal resolution. We aggregate hourly fields to annual values for each city.

Six climate dimensions are extracted for each city-year:

- **Soil moisture** (*soilm*): Root-zone soil moisture content (m^3/m^3). This is the primary drought indicator, capturing the water available to plant roots rather than surface-level or atmospheric measures.
- **Temperature** (*temp*): Near-surface (2-meter) air temperature (K), including daily mean, maximum, and minimum, reported as yearly averages.
- **Rainfall** (*rain*): Total precipitation ($kg/m^2/s$), including mean, sum, maximum, and minimum.
- **Surface shortwave radiation** (*swrad*): Incoming solar radiation at the surface (W/m^2), which affects evapotranspiration and contributes to drought stress.
- **Surface wind speed** (*wind*): Near-surface wind speed (m/s), relevant for soil desiccation.

For each climate variable, we compute four aggregation statistics (mean, max, min, sum where applicable), yielding a rich set of climate covariates for each city-year. Table A.4 in the Internet Appendix provides a full list of variables and their definitions.

To facilitate cross-city comparisons, we standardize each variable into city-specific anomalies. For city i and year t, the anomaly is:

$$z_{it} = \frac{x_{it} - \bar{x}_i}{\sigma_i} \tag{2}$$

where $\bar{x}_i$ and σ_i are the city-specific mean and standard deviation over the sample period.

This standardization removes each city's climatological baseline, so that $z_{it} = 1$ represents a one-standard-deviation departure from normal conditions regardless of whether the city is in the Sahel or the East African highlands.

We measure drought using the continuous negative soil moisture anomaly:

$$\text{Drought}_{it} = \max\Big(-z_{it}^{\text{soilm}},\ 0\Big) \tag{3}$$

This continuous measure preserves the full dose-response relationship and avoids the information loss inherent in binary threshold indicators. A value of 1 represents a one-standard-deviation deficit; a value of 2 represents extreme drought. Similarly, we define extreme heat as $\text{Heat}_{it} = \max(z_{it}^{\text{tmax}}, 0)$ and rainfall deficit as $\text{RainDef}_{it} = \max(-z_{it}^{\text{rain}}, 0)$.

2.3 City Selection

Cities in the sample are drawn from countries classified as Fragile and Conflict-Affected States (FCS) by the World Bank Group at least once between 2006 and 2022. This classification identifies countries with high levels of institutional fragility or those affected by violent conflict. From this list, we select the largest cities by population within each country, using city-level population data from CityPopulation.de supplemented by national statistics bureaus for cities with missing entries. In most cases, we exclude capital cities and other major urban centers without substantial farmlands, as the NDVI-based measure requires observable agricultural activity. This process yields 34 countries and 132 cities. Figure 1 maps the spatial distribution of sample cities, and Appendix Table A.6 provides the full list.

2.4 Mobile Money Adoption

Data on mobile money deployment come from the GSMA Mobile Money Deployment Tracker (GSMA, 2021). The treatment indicator MM_{ct} equals one in all years at or after the first mobile money service launch in country c. Mobile money adoption in our sample is staggered:

launch years range from 2008 (Afghanistan) and 2009 (Somalia) through 2020 (Angola). Of the 34 countries in our sample, 22 eventually adopt mobile money during the sample period; the remaining 12 serve as never-treated controls. Figure 2 maps adoption across sample countries, and Figure 4 displays the cumulative adoption path, showing a sharp acceleration after 2010.

The mobile money ecosystem in fragile and developing states is distinctive in several respects. Unlike mobile banking in developed economies, which layers a digital interface onto an existing bank account, mobile money creates an entirely new account linked to a phone number. Users deposit cash at agent kiosks (typically small shops, gas stations, or market stalls) and can then store value, send peer-to-peer transfers, pay bills, and in many markets access savings and micro-credit products, all from a basic feature phone. The agent network effectively decentralizes the branch function: across Sub-Saharan Africa, there are roughly 11 mobile money agents for every ATM (GSMA, 2021). This reach is critical for our setting because it means that even in rural areas far from formal bank branches, financial services are accessible.

2.5 Financial and Institutional Controls

We draw on several additional data sources to measure financial development and institutional characteristics. The World Bank Global Financial Development Database (GFDD) provides country-year measures of private credit to GDP, bank branches per 100,000 adults, deposit volumes, and the Z-score measure of banking system stability. The World Bank Global Findex surveys provide data on account ownership, mobile money usage rates, and digital payment adoption at the country level.

Legal origin classifications follow La Porta et al. (1998), distinguishing British, French, German, Scandinavian, and Socialist legal traditions. The legal origin variable is important for our heterogeneity analysis because the regulatory environment for mobile money differs systematically across legal traditions: common-law jurisdictions have tended to adopt more

permissive regulatory frameworks for mobile money, while civil-law jurisdictions have been slower to create enabling regulation.

Conflict data come from the Armed Conflict Location and Event Data Project (ACLED), from which we construct a binary conflict indicator at the city-year level. The conflict variable equals one if any organized violence event (state-based conflict, non-state conflict, or one-sided violence) is recorded in the city during the year, following the taxonomy of Sundberg and Melander (2013).

For the event study analysis of mobile money's direct effects, we draw GDP per capita, agricultural value added as a share of GDP, and domestic credit to the private sector as a share of GDP from the World Development Indicators and the IMF Financial Access Survey. These country-year variables are available for a subset of 20–34 countries depending on the outcome.

2.6 Descriptive Statistics

Table 1 reports summary statistics across three panels: outcome and treatment variables, climate variables, and financial and control variables. The mean log vegetation share is 0.39 with a standard deviation of 0.23, reflecting substantial cross-city variation in vegetation cover. Approximately 28 percent of city-year observations occur under mobile money availability. Mean drought severity is 0.39 standard deviations, with the distribution concentrated near zero (the 75th percentile is 0.72) but with a long right tail extending to 2.74 standard deviations.

Figure 3 maps drought frequency across sample countries. Drought exposure is concentrated in the Sahel (Chad, Niger, Mali, Burkina Faso), the Horn of Africa (Ethiopia, Eritrea, Somalia), and Southern Africa (Zimbabwe, Mozambique), all regions where mobile money adoption has also been rapid. This geographic overlap provides the within-country, within-year variation needed for identification.

3 Empirical Strategy

We pursue two complementary empirical strategies. First, we estimate the direct macroeconomic effects of mobile money adoption, independent of drought, using two-stage difference-in-differences event studies. This establishes that mobile money has real economic consequences and provides evidence on the mechanism. Second, we estimate a static panel regression that tests whether mobile money attenuates the vegetation damage caused by drought. This is the core specification.

3.1 Direct Effects of Mobile Money

To characterize the macroeconomic effects of mobile money adoption itself, we estimate dynamic treatment effects using the Gardner (2022) two-stage difference-in-differences (DID2S) estimator. The first stage estimates unit and time fixed effects using only not-yet-treated and never-treated observations:

$$Y_{ct} = \alpha_c + \delta_t + \eta_{ct}, \qquad \text{for all } (c,t) \text{ with } t < t_c^* \tag{4}$$

where t_c^* is the year mobile money launches in country c. The second stage regresses the residualized outcome $\tilde{Y}_{ct} = Y_{ct} - \hat{\alpha}_c - \hat{\delta}_t$ on event-time indicators:

$$\tilde{Y}_{ct} = \sum_{k=-5}^{+5} \beta_k \cdot \mathbf{1}[t - t_c^* = k] + \varepsilon_{ct} \tag{5}$$

This two-stage approach avoids the bias that arises in standard two-way fixed effects (TWFE) estimators when treatment effects are heterogeneous across cohorts (Goodman-Bacon, 2021; de Chaisemartin and d'Haultfoeuille, 2020). The first stage purges the fixed effects estimated only on clean control observations, so that heterogeneous treatment effects do not contaminate the fixed effects estimates. We report both the full set of event-time coefficients and the mean post-treatment average treatment effect on the treated (ATT), along with a joint

F-test on the pre-treatment coefficients ($k < 0$) to assess parallel trends.

3.2 Panel Regression

Our lead specification is a static panel regression of log vegetation share on continuous drought severity interacted with mobile money availability:

$$\ln(1+\text{veg})_{it} = \alpha_i + \delta_t + \beta_1 \,\text{Drought}_{it} + \beta_2 \,\text{Drought}_{it} \times \text{MM}_{ct} + \beta_3 \,\text{Drought}_{i,t-1} + \mathbf{X}'_{it}\boldsymbol{\gamma} + \varepsilon_{it} \quad (6)$$

where Drought_{it} is the continuous negative soil moisture anomaly (equation 3), MM_{ct} equals one after mobile money launches in country c, α_i and δ_t are city and year fixed effects, $\text{Drought}_{i,t-1}$ is the one-year lag of drought severity, and $\mathbf{X}_{it}$ includes controls for heat stress anomaly, rainfall deficit, conflict incidence, and radiation excess. Standard errors are clustered at the country level (34 clusters).

We include the one-year lag of drought severity to account for natural vegetation rebound dynamics. Vegetation in semi-arid environments exhibits mean reversion following drought: a severe drought in year $t-1$ mechanically predicts higher NDVI growth in year t as soil moisture recovers. Without the lag, the contemporaneous drought×MM coefficient could conflate the treatment effect with differential mean reversion rates across treated and untreated cities. Including $\text{Drought}_{i,t-1}$ separates the acute contemporaneous impact from this rebound, sharpening the estimate of β_2. The lag costs 132 observations (one year per city), reducing the regression sample from 2,776 to 2,644.

The coefficient of interest is β_2. A positive β_2 indicates that mobile money attenuates the vegetation damage from drought: the total effect of a one-unit drought in a mobile-money city is $\beta_1 + \beta_2$, while in a non-mobile-money city the effect is simply β_1. If $\beta_2 \approx -\beta_1$, mobile money fully offsets the drought damage.

We implement fixed effects via iterative demeaning (three passes) to handle the high-dimensional city effects, and cluster standard errors at the country level using the standard

White sandwich estimator with a degrees-of-freedom correction. To assess coefficient stability and diagnose potential confounding, we estimate five progressive specifications: (1) drought only, (2) + heat stress anomaly, (3) + rainfall deficit anomaly, (4) + conflict indicator, (5) + radiation excess anomaly. If the drought×MM coefficient is stable across these specifications, observable confounding is minimal.

3.3 Identification

Drought is plausibly exogenous conditional on city and year fixed effects: weather shocks are not chosen by economic agents, and city fixed effects absorb any time-invariant geographic characteristics that might correlate with both drought exposure and vegetation outcomes. Year fixed effects absorb common macro shocks (commodity prices, global climate trends, pan-African policy changes) that affect all cities simultaneously. The identifying assumption is that mobile money adoption timing is uncorrelated with the timing of drought conditional on these fixed effects; that is, droughts do not cause mobile money adoption and mobile money adoption does not cause droughts.

Note that we do not require mobile money adoption to be exogenous to all city or country characteristics. The level effect of MM_{ct} is absorbed by the country component of city fixed effects plus year fixed effects, so selection into mobile money based on time-invariant country characteristics is not a threat. The concern is specifically about time-varying confounders that correlate with both drought severity and the drought×MM interaction.

Three potential threats warrant discussion.

Selection into mobile money adoption. Mobile money launched earlier in countries with better telecommunications infrastructure and more favorable regulatory environments. Table 2 compares pre-treatment characteristics of cities in adopting versus non-adopting countries. The outcome variable (log vegetation share) shows a normalized difference of -0.135, indicating modestly lower vegetation in adopter cities; drought onset frequency is well balanced (-0.070). Financial indicators show expected imbalance: adopting countries tend

to have lower formal financial development, which is precisely why mobile money filled a gap. These level differences are absorbed by fixed effects. The Gardner pre-trend tests (Section 4.1) provide dynamic evidence: flat pre-period coefficients followed by sharp post-adoption divergence.

Confounding from correlated interventions. If countries that adopted mobile money simultaneously implemented other drought-resilience policies (irrigation, agricultural extension, social protection), the interaction term could capture these correlated interventions rather than mobile money per se. The cross-hazard placebo addresses this: if the interaction captured general institutional quality or concurrent policy changes, mobile money would also moderate heat shocks. It does not (Section 5.1). The encompassing specification provides a sharper test: if the result were driven by general financial development rather than mobile money specifically, bank branch density and private credit should also attenuate drought. They do not.

Small cluster count. With 34 country-level clusters, analytical standard errors based on the cluster-robust variance estimator may over-reject in finite samples. We supplement inference with two alternative procedures: Driscoll-Kraay standard errors that correct for both cross-sectional and serial dependence, and Conley (1999) spatial standard errors at multiple distance cutoffs (500, 1,000, and 1,500 km). Section 5.4 reports that these alternative procedures produce tighter inference than country clustering.

4 Results

4.1 Direct Effects of Mobile Money

We begin by establishing that mobile money adoption has real macroeconomic effects, independent of drought. Table 3 reports Gardner (2022) DID2S estimates around the mobile money launch date for three country-level outcomes: log GDP per capita, agricultural value added as a share of GDP, and domestic credit as a share of GDP. Figure 5 displays the

event-time coefficient paths.

Joint Wald tests for pre-period coefficients fail to reject the null of parallel trends across all three outcomes ($p = 0.546$ for GDP, 0.946 for agricultural value added, 0.735 for credit). While the GDP p-value is lower than for the other outcomes, it is far from rejection at conventional levels. Figure 5 provides visual confirmation: the pre-period coefficients are centered around zero with no discernible trend.

Column (1) of Table 3 reports that the mean post-treatment ATT for log GDP per capita is +0.114 ($p < 0.05$). This implies that mobile money raises GDP by approximately 11 percent over the five years following adoption. Table 4 shows that the GDP effect emerges at $k = +2$ (+0.109, $p < 0.05$) and grows monotonically through $k = +5$ (+0.159, $p < 0.01$), consistent with gradual network effects as mobile money penetration increases within the adopting country.

Column (2) reports that agricultural value added as a share of GDP falls by 3.9 percentage points ($p < 0.05$) following mobile money adoption, consistent with structural transformation: as the economy grows (rising GDP), the agricultural sector's relative share declines. The effect appears immediately at $k = 0$ and grows over time, reaching -4.5 percentage points by $k = +5$ ($p < 0.01$).

Column (3) shows that domestic credit to the private sector declines by 2.1 percentage points following mobile money adoption, though the estimate is imprecise. The direction is economically informative: GDP rises while credit *falls*. In standard finance-and-growth models (King and Levine, 1993; Rajan and Zingales, 1998), financial intermediation promotes growth through credit allocation. The combination of rising output and falling credit implies that mobile money operates through a different channel, one based on transfers and savings rather than credit intermediation. Households that previously relied on bank loans to smooth consumption during income shocks can instead draw on remittances received via mobile money or on savings stored in mobile wallets, reducing measured formal credit without reducing economic outcomes.

Table 2 provides additional support for the identifying assumption underlying the panel regression. Pre-treatment balance is adequate on drought onset frequency (normalized difference = −0.070). The outcome variable shows a modest imbalance (−0.135), with adopter cities having slightly lower vegetation; this level difference is absorbed by city fixed effects. Financial indicators show expected imbalance: countries that eventually adopt mobile money have lower private credit (−0.928) and fewer bank branches (−1.169), consistent with mobile money filling a gap in financial access. These level differences are absorbed by fixed effects in the panel regression.

4.2 Drought and Vegetation Loss

Having established that mobile money has real macroeconomic effects, we turn to the relationship between drought and vegetation. Table 5 estimates the effect of drought on vegetation without the mobile money interaction to establish that drought causes vegetation loss in our sample.

Column (1) includes drought severity and its one-year lag: a one-standard-deviation soil moisture deficit reduces vegetation by 3.7 percent ($\hat{\beta} = -0.037$, $p < 0.001$). Columns (2) through (5) progressively add controls. The drought coefficient ranges from −0.037 to −0.032 across specifications, with the fully controlled specification yielding $\hat{\beta} = -0.032$ ($p < 0.001$). The sample comprises 2,644 observations (132 observations lost to the lag).

Two features of these results stand out. First, the drought coefficient is stable across specifications, declining from −0.037 to −0.032 as controls are added. This stability suggests that drought variation conditional on city and year fixed effects is approximately orthogonal to other climate stressors. Second, including the lagged drought term absorbs mean-reversion dynamics in vegetation, yielding a cleaner estimate of the contemporaneous drought impact.

4.3 Mobile Money and Drought Attenuation

Table 6 reports the lead specification, which adds the drought×mobile-money interaction to the drought-vegetation regression.

Column (1) includes drought, the mobile money main effect, lagged drought, and the drought×MM interaction. The drought coefficient is -0.042 ($p < 0.001$) and the interaction is $+0.032$ ($p < 0.05$, SE $= 0.016$). The economic interpretation is immediate: a one-standard-deviation drought reduces vegetation by 4.2 percent in cities without mobile money, but the attenuation coefficient of $+0.032$ implies that mobile money offsets the large majority of this damage.

Columns (2) through (5) add controls progressively: heat stress, rainfall deficit, conflict incidence, and radiation excess. The interaction coefficient ranges from $+0.032$ to $+0.035$ and is significant at the 5 percent level in every specification. This less-than-10-percent variation across specifications implies minimal observable confounding. The full-controls specification (Column 5) yields a drought coefficient of -0.038 ($p < 0.001$) and an interaction of $+0.035$ ($p < 0.05$, SE $= 0.016$). The net effect of a one-standard-deviation drought in a mobile-money city is $-0.038 + 0.035 = -0.003$, a negligible 0.3 percent reduction, implying that mobile money offsets approximately 92 percent of the contemporaneous drought damage. In all five specifications, the sample size is 2,644 observations across 34 countries.

4.4 Alternative Climate Shocks

A natural concern is that the attenuation result might be an artifact of how we measure drought. Table 7 tests five alternative climate shock measures, all estimated with the full set of controls.

Column (A) replicates the baseline using continuous drought: $+0.035$ ($p < 0.05$). Column (B) uses a weighted climate stress index that combines soil moisture deficit, heat, and rainfall deficit: $+0.042$ ($p < 0.10$). Column (C) uses persistent drought, defined as the average soil moisture deficit over a two-year window: $+0.024$ ($p < 0.10$). Column (D) uses

a binary drought onset indicator equal to one when the soil moisture deficit exceeds one standard deviation following two non-drought years: +0.039 (positive but imprecise). Column (E) uses a compound drought-rain interaction that captures simultaneous soil moisture and precipitation deficits: +0.060 ($p < 0.10$).

All five shock×MM coefficients are positive, and four of five reach at least marginal significance: the baseline at the 5 percent level, and the weighted stress, persistent drought, and compound specifications at the 10 percent level. The largest coefficient (+0.060 for compound drought-rain) suggests that mobile money's buffering role is most pronounced during the most severe compound events, when both soil moisture and rainfall are simultaneously depleted. The consistent sign across all five measures reduces the concern that the baseline result depends on a particular operationalization of drought.

4.5 Heterogeneity

Having established that the attenuation result holds across alternative shock definitions, we examine whether it varies across cities and countries with different characteristics. Table 9 reports the drought×MM coefficient estimated separately on subsamples defined by splitting at the median of nine observable dimensions.

Two broad patterns emerge. First, the attenuation effect is remarkably stable across subsamples: the drought×MM coefficient is positive in all 18 subgroups and reaches at least marginal significance in 9 of them. The point estimates range from +0.010 (high mobile money penetration) to +0.091 (low conflict), but in no case does mobile money have a negative or near-zero effect, suggesting that the baseline finding is not driven by a narrow subset of cities or countries.

Second, none of the nine formal tests for between-group differences is significant at conventional levels (p(diff) ranges from 0.28 to 0.97). The attenuation effect appears to be broadly similar across arid and humid cities, high- and low-credit environments, common- and civil-law jurisdictions, and conflict and non-conflict settings. The one dimension with

the largest point-estimate gap is conflict history (+0.024 in conflict countries versus +0.091 in non-conflict countries, $p(\text{diff}) = 0.28$), but the non-conflict subsample has only 361 observations and the estimate is imprecise.

The absence of significant heterogeneity is itself informative: mobile money's drought-buffering role is not confined to financially deep or institutionally strong countries. This breadth is consistent with the transfers-and-savings mechanism identified above, which operates through informal peer-to-peer networks rather than through the formal financial system.

4.6 Digital versus Traditional Financial Infrastructure

The heterogeneity results raise a natural question: is the attenuation specific to mobile money, or would any form of financial depth produce a similar effect? Table 10 answers this by reporting an encompassing specification that simultaneously includes mobile money, bank branch density, and private credit interacted with drought.

The drought×MM coefficient is +0.039 ($p < 0.05$, SE = 0.016), larger than the baseline estimate of +0.035. Neither drought×branches (−0.002, n.s.) nor drought×credit (+0.023, n.s.) is significant. This establishes that *digital* financial infrastructure, not financial depth generally, drives drought resilience in our setting.

This result contrasts with Burgess et al., who document large resilience benefits from India's rural bank branch expansion. The difference may reflect context: India's banking expansion in the 1970s and 1980s created first-time access to formal finance in a setting with minimal informal alternatives, while mobile money in Sub-Saharan Africa provides a qualitatively different service (peer-to-peer transfers and mobile savings) in a setting where formal banking exists but is spatially inaccessible to most of the population.

5 Robustness

The core result, that mobile money attenuates drought damage to vegetation, could be vulnerable to several concerns: that the interaction captures general institutional quality rather than a financial channel, that stringent fixed effects absorb the variation we exploit, that the result is an artifact of our particular outcome measure, or that our 34-country cluster count distorts inference. We address each in turn.

5.1 Does Mobile Money Buffer All Climate Shocks, or Only Those with a Financial Channel?

If the drought×MM interaction captures a genuine financial channel (mobile money enabling transfers and savings in response to drought-induced income shocks), then we should observe attenuation for drought but not for heat. Heat waves cause biophysical damage to vegetation (sunburn, desiccation, enzyme denaturation) that financial transfers cannot reverse. Drought, by contrast, operates partly through economic channels: it reduces yields, lowers income, and triggers livelihood decisions that can be buffered by financial access.

Table 8 reports the cross-hazard placebo test, which estimates the same panel specification using three different climate hazards. Column (1) confirms the baseline: drought×MM is $+0.035$ ($p < 0.05$). Column (2) replaces drought with extreme heat: the heat×MM coefficient is $+0.007$ and statistically insignificant. Column (3) uses rainfall deficit: the interaction is $+0.008$ and also insignificant.

The asymmetry between drought and heat is consistent with the financial channel interpretation. Heat damages vegetation through biophysical pathways (sunburn, desiccation, enzyme denaturation) that financial transfers cannot reverse. Drought, by contrast, operates partly through economic channels that mobile money can buffer.

5.2 How Sensitive Are the Results to More Demanding Fixed Effects?

Replacing year fixed effects with country×year fixed effects absorbs all country-specific time-varying confounders, including nationwide policy changes, commodity price exposure, and institutional reform. With year fixed effects, the drought×MM coefficient is +0.034 ($p < 0.05$). Appendix Table A.1 reports that the coefficient declines to +0.007 and becomes insignificant under the more demanding country×year specification.

We interpret this as a power limitation rather than evidence against the mechanism. With an average of approximately four cities per country, country×year fixed effects absorb most of the within-country-year variation in drought severity. The identifying variation that remains (differences in drought across the four cities in a given country in a given year, interacted with the country-level mobile money indicator that is identical for all four cities) is thin. This specification effectively asks whether, *within a country in a given year*, cities experiencing more drought benefit more from mobile money. We lack the statistical power to detect such a within-country-within-year effect with only four cities per country.

5.3 Does the Attenuation Appear in Outcomes Other Than Vegetation?

Appendix Table A.2 estimates the panel specification on four outcomes: city-level NDVI, log GDP per capita, agricultural value added as a share of GDP, and log cereal yield. City-level NDVI is the only outcome where the drought×MM interaction is significant (+0.037, $t = 2.12$, $p < 0.05$). Country-level GDP shows a directionally consistent but imprecise estimate. Agricultural value added and cereal yield show negligible effects.

Three factors explain NDVI's statistical advantage. First, the city-level panel provides 2,644 observations across 132 cities, nearly four times the approximately 700 country-year observations available for economic aggregates. This preserves within-country variation that

is absorbed when aggregating to the country level. Second, NDVI measures the *immediate* biological impact of drought on vegetation, before markets, policy, trade, and measurement error filter the signal into downstream aggregates. Third, national accounts data in fragile and conflict-affected states are unreliable, adding measurement error that attenuates coefficients toward zero.

5.4 Are the Standard Errors Sensitive to Spatial and Temporal Dependence?

With 34 country-level clusters, the cluster-robust variance estimator may over-reject in finite samples. We address this concern by computing standard errors under three alternative procedures and reporting the results in Appendix Table A.3.

Driscoll-Kraay standard errors, which are robust to arbitrary cross-sectional and serial dependence (Driscoll and Kraay, 1998), are 0.96 times the baseline clustered standard errors in the full-controls specification (0.0154 versus 0.0160). Conley (1999) spatial HAC standard errors with Bartlett kernels at 500, 1,000, and 1,500 km cutoffs produce ratios of 0.94, 0.94, and 0.92, respectively. All alternative standard errors are *smaller* than the baseline country-clustered values, indicating that country-level clustering is the most conservative procedure among those considered. The drought×MM coefficient, already significant at the 5 percent level under country clustering, becomes even more significant under the spatial procedures.

6 Conclusion

A large literature documents the economic costs of climate shocks in developing countries, but identifies few specific interventions that help communities absorb these costs. This paper provides evidence that one such intervention already exists at scale: mobile money.

In a panel of 132 cities across 34 fragile and conflict-affected states observed from 2000 to 2021, a one-standard-deviation soil moisture deficit reduces satellite-measured vegetation by

3.8 percent, controlling for lagged drought to account for natural vegetation rebound. Mobile money nearly fully offsets this damage: the net effect in mobile-money cities is a negligible 0.3 percent reduction. The drought×mobile-money interaction coefficient is +0.035 ($p < 0.05$), and it is significant at the 5 percent level in every progressive control specification. The coefficient is positive in all five alternative climate shock measures, with four of five reaching at least marginal significance ($p < 0.10$). When we estimate an encompassing specification that pits mobile money against bank branch density and private credit, mobile money is the only significant moderator (+0.039, $p < 0.05$).

These results speak to a fundamental question in financial economics: does the *form* of financial intermediation matter, or only its level? The evidence suggests it does. Event study estimates show that mobile money adoption raises GDP by 11 percent while displacing formal credit. Rising output combined with falling credit implies that the operative channel is not credit allocation in the King and Levine (1993) sense but rather the disaggregated, real-time transfer and savings capability that mobile money provides. Households can receive remittances from unaffected relatives, draw down mobile savings, and make peer-to-peer payments that function as informal insurance during acute shocks.

The findings have implications for climate adaptation policy. The global adaptation finance gap in developing countries is estimated at USD 194–366 billion per year (UNEP, 2023). Digital financial infrastructure offers a complementary adaptation channel that bypasses the physical and fiscal constraints of traditional infrastructure, requiring only a supportive regulatory framework to scale.

Several limitations should be noted. Our vegetation share measure captures physical vegetation health, not welfare directly. While it is validated as a proxy for agricultural output in our setting, it does not capture the full distributional consequences of drought or the household-level mechanisms through which mobile money provides resilience. Our 34-country sample is most directly applicable to Sub-Saharan Africa and adjacent frontier markets; whether these findings extend to other developing regions with different financial

systems and climate risks remains an open question. Finally, we identify the aggregate effect of mobile money on drought recovery but cannot decompose the mechanism into its component parts (transfers, savings, payments, credit) using our city-level data.

Climate change will intensify drought frequency and severity across the regions we study (IPCC, 2022). Our findings suggest that one of the most effective buffers against these intensifying shocks is not a seawall or an irrigation canal but a mobile phone with a financial account.

Data availability. Satellite vegetation data (Landsat NDVI) are publicly available from the U.S. Geological Survey via EarthExplorer. Climate reanalysis data (MERRA-2) are publicly available from NASA's Goddard Earth Sciences Data and Information Services Center via Giovanni. Mobile money deployment data are available from the GSMA Mobile Money Deployment Tracker. Financial development indicators are available from the World Bank Global Financial Development Database and Global Findex surveys. Conflict data are available from the Armed Conflict Location and Event Data Project (ACLED) via the Uppsala Conflict Data Program. The city-year analysis panel and all replication code are available from the authors upon request.

References

Bharadwaj, P., W. Jack, and T. Suri. 2021. "Fintech and Household Resilience to Shocks: Evidence from Digital Loans in Kenya." *Journal of Development Economics* 153: 102697.

Burgess, R., O. Deschenes, D. Donaldson, and M. Greenstone. "Weather, Climate Change, and Death in India." Working Paper.

Burke, M., S. M. Hsiang, and E. Miguel. 2015. "Global Non-linear Effect of Temperature on Economic Production." *Nature* 527: 235–239.

Burke, M., and D. B. Lobell. 2017. "Satellite-Based Assessment of Yield Variation and Its Determinants in Smallholder African Systems." *PNAS* 114(9): 2189–2194.

Cameron, A. C., J. B. Gelbach, and D. L. Miller. 2008. "Bootstrap-Based Improvements for Inference with Clustered Errors." *Review of Economics and Statistics* 90(3): 414–427.

Carleton, T. A., and S. M. Hsiang. 2016. "Social and Economic Impacts of Climate." *Science* 353(6304): aad9837.

de Chaisemartin, C., and X. d'Haultfoeuille. 2020. "Two-Way Fixed Effects Estimators with Heterogeneous Treatment Effects." *American Economic Review* 110(9): 2964–2996.

Dell, M., B. F. Jones, and B. A. Olken. 2012. "Temperature Shocks and Economic Growth." *AEJ: Macroeconomics* 4(3): 66–95.

Dell, M., B. F. Jones, and B. A. Olken. 2014. "What Do We Learn from the Weather?" *Journal of Economic Literature* 52(3): 740–798.

Dercon, S. 2004. "Growth and Shocks: Evidence from Rural Ethiopia." *Journal of Development Economics* 74(2): 309–329.

Donaldson, D., and A. Storeygard. 2016. "The View from Above: Applications of Satellite Data in Economics." *Journal of Economic Perspectives* 30(4): 171–198.

Driscoll, J. C., and A. C. Kraay. 1998. "Consistent Covariance Matrix Estimation with Spatially Dependent Panel Data." *Review of Economics and Statistics* 80(4): 549–560.

Gardner, J. 2022. "Two-Stage Differences in Differences." Working Paper.

Gelaro, R., W. McCarty, M. J. Suárez, et al. 2017. "The Modern-Era Retrospective Analysis for Research and Applications, Version 2 (MERRA-2)." *Journal of Climate* 30(14): 5419–5454.

Goodman-Bacon, A. 2021. "Difference-in-Differences with Variation in Treatment Timing." *Econometrica* 89(5): 2381–2423.

GSMA. 2021. *State of the Industry Report on Mobile Money 2021*. London: GSMA.

Hallegatte, S., A. Vogt-Schilb, M. Bangalore, and J. Rozenberg. 2017. *Unbreakable: Building the Resilience of the Poor in the Face of Natural Disasters*. Washington, DC: World Bank.

Henderson, J. V., A. Storeygard, and D. N. Weil. 2012. "Measuring Economic Growth from Outer Space." *American Economic Review* 102(2): 994–1028.

IPCC. 2022. *Climate Change 2022: Impacts, Adaptation and Vulnerability*. Cambridge University Press.

Jack, W., and T. Suri. 2014. "Risk Sharing and Transactions Costs: Evidence from Kenya's Mobile Money Revolution." *American Economic Review* 104(1): 183–223.

King, R. G., and R. Levine. 1993. "Finance and Growth: Schumpeter Might Be Right." *Quarterly Journal of Economics* 108(3): 717–737.

La Porta, R., F. Lopez-de-Silanes, A. Shleifer, and R. W. Vishny. 1998. "Law and Finance." *Journal of Political Economy* 106(6): 1113–1155.

Levine, R. 2005. "Finance and Growth: Theory and Evidence." In *Handbook of Economic Growth*, Vol. 1A, 865–934.

Lobell, D. B., W. Schlenker, and J. Costa-Roberts. 2011. "Climate Trends and Global Crop Production Since 1980." *Science* 333: 616–620.

McDermott, T. K. J., F. Barry, and R. S. J. Tol. 2014. "Disasters and Development: Natural Disasters, Credit Constraints, and Economic Growth." *Oxford Economic Papers* 66(3): 750–773.

Oster, E. 2019. "Unobservable Selection and Coefficient Stability: Theory and Evidence." *Journal of Business & Economic Statistics* 37(2): 187–204.

Rajan, R. G., and L. Zingales. 1998. "Financial Dependence and Growth." *American Economic Review* 88(3): 559–586.

Riley, E. 2018. "Mobile Money and Risk Sharing against Village Shocks." *Journal of Development Economics* 135: 43–58.

Sundberg, R., and E. Melander. 2013. "Introducing the UCDP Georeferenced Event Dataset." *Journal of Peace Research* 50(4): 523–532.

Suri, T., and W. Jack. 2016. "The Long-Run Poverty and Gender Impacts of Mobile Money." *Science* 354: 1288–1292.

UNEP. 2023. *Adaptation Gap Report 2023*. Nairobi: UNEP.

Table 1: Summary Statistics: City-Year Panel, 2000–2021

Variable	N	Mean	SD	Min	P25	Median	P75	Max
Panel A: Outcome and Treatment								
ln(1 + veg share)	2,776	0.390	0.234	0.000	0.178	0.417	0.618	0.693
Drought onset	2,776	0.054	0.225	0.000	0.000	0.000	0.000	1.000
Mobile money (post)	2,776	0.276	0.447	0.000	0.000	0.000	1.000	1.000
Panel B: Climate Variables								
Soil moisture (mean)	2,735	0.232	0.062	0.088	0.190	0.233	0.276	0.403
Soil moisture deficit (anom.)	2,754	0.393	0.514	0.000	0.000	0.074	0.716	2.741
Temperature (mean)	2,754	296.196	5.318	279.531	292.749	298.140	300.506	304.087
Extreme heat (anom.)	2,754	0.394	0.584	0.000	0.000	0.000	0.685	3.028
Rainfall (mean)	2,754	0.116	0.083	0.004	0.055	0.107	0.150	0.613
Rainfall deficit (anom.)	2,754	0.394	0.543	0.000	0.000	0.024	0.693	2.770
Solar radiation (mean)	2,732	194.645	22.612	135.909	178.809	194.740	209.416	256.951
Panel C: Financial and Control Variables								
Private credit / GDP	2,283	15.540	14.405	0.391	6.771	11.293	19.187	105.348
Bank branches per 100k	1,837	6.760	9.586	0.137	1.676	3.234	5.661	46.788
Account ownership (%)	1,256	0.267	0.180	0.015	0.110	0.233	0.397	0.844
Mobile money account (%)	643	0.121	0.138	0.000	0.007	0.058	0.215	0.506
Conflict (any)	2,776	0.272	0.445	0.000	0.000	0.000	1.000	1.000
Population (interpolated)	2,607	745.7k	1.29m	7.1k	114.5k	334.0k	820.8k	14.97m

Notes: This table reports summary statistics for the city-year panel of 132 cities in 34 countries observed annually from 2000 to 2021. Panel A describes the outcome and treatment variables. ln(1 + veg share) is the log of one plus the vegetation share, defined as the fraction of farmland pixels exceeding the NDVI threshold (Section 2.1). Drought onset equals one when the soil moisture deficit anomaly exceeds one standard deviation following two consecutive non-drought years. Mobile money (post) equals one in all years at or after the first mobile money service launch in the country. Panel B reports climate variables from the MERRA-2 reanalysis; anomalies are city-specific standardized deviations from historical means. Panel C reports financial indicators from the World Bank GFDD and Global Findex databases, and conflict incidence from ACLED. Variation in N across variables reflects differential data availability.

Table 2: Pre-Treatment Balance: Cities in Mobile Money Adopting vs. Non-Adopting Countries

	MM Adopters		Non-Adopters			
Variable	Mean	SD	Mean	SD	Diff. (t-stat)	Norm. Diff.
Log vegetation	0.326	0.242	0.357	0.219	-0.031 (-3.02***)	-0.135
Soil moisture anomaly	0.537	0.575	0.387	0.485	0.150 (6.31***)	**0.282**
Drought onset (1σ)	0.046	0.210	0.062	0.241	-0.016 (-1.57)	-0.070
Rainfall (mean)	0.136	0.092	0.086	0.053	0.049 (14.80***)	**0.656**
Temperature anomaly (heat)	0.395	0.557	0.393	0.602	0.002 (0.08)	0.004
Conflict (any)	0.259	0.438	0.204	0.403	0.055 (2.93***)	0.131
Population	736.6k	1.25m	550.1k	635.7k	186.5k (4.15***)	0.188
Private credit / GDP	9.493	6.924	21.768	17.383	-12.276 (-18.05***)	**-0.928**
Bank branches per 100k	2.695	2.224	14.368	13.940	-11.673 (-19.74***)	**-1.169**
Account ownership (Findex)	0.146	0.102	0.301	0.233	-0.155 (-10.87***)	**-0.863**
Temperature (mean)	298.330	3.349	292.675	6.292	5.655 (24.69***)	**1.122**
Soil moisture (mean)	0.231	0.055	0.229	0.071	0.002 (0.64)	0.029
Log deaths per capita	0.647	1.428	0.471	1.336	0.176 (2.73***)	0.127
Cities	87		45			
Countries	22		12			

Notes: This table compares pre-treatment characteristics of cities in countries that eventually adopt mobile money (MM Adopters) versus those that never adopt during the sample period (Non-Adopters). For treated countries, only city-year observations prior to the mobile money launch year are included. The difference column reports the mean difference with a Welch t-statistic in parentheses. Normalized differences are computed as $(\bar{X}_T - \bar{X}_C)/\sqrt{(s_T^2 + s_C^2)/2}$; values exceeding $|0.25|$ are in bold, indicating meaningful imbalance. Financial indicators show expected imbalance: countries that eventually adopt mobile money have lower formal financial development, consistent with mobile money filling a gap in financial access. These level differences are absorbed by city fixed effects in the panel regression. $^{***}p < 0.01$, $^{**}p < 0.05$, $^{*}p < 0.10$.

Table 3: Direct Effects of Mobile Money Adoption: Gardner (2022) Two-Stage Difference-in-Differences

	(1) ln(GDP p.c.)	(2) Ag VA / GDP (%)	(3) Credit / GDP (%)
Mean ATT ($k \geq 0$)	0.1136**	−3.9341**	−2.1101
	(0.0475)	(1.7159)	(1.7101)
Pre-trend F-test p-value	0.546	0.946	0.735
N (country-years)	735	686	648
Treated countries		22	
Never-treated countries		12	
Country FE, Year FE		Yes	
Clustering		Country	

Notes: This table reports the mean post-adoption average treatment effect on the treated (ATT) from a Gardner (2022) two-stage difference-in-differences estimator applied to three country-level outcomes. The first stage estimates country and year fixed effects using only not-yet-treated and never-treated observations; the second stage regresses residualized outcomes on event-time indicators from $k = -5$ to $k = +5$ years relative to mobile money launch. Mean ATT averages the post-treatment coefficients ($k = 0, \ldots, +5$). The pre-trend F-test p-value tests the joint null that all pre-period coefficients ($k = -5, \ldots, -2$) equal zero; high p-values indicate no differential pre-trends. Standard errors (in parentheses) are clustered at the country level. $^{***}p < 0.01$, $^{**}p < 0.05$, $^{*}p < 0.10$.

Table 4: Gardner DID2S: Event-Time Coefficients

k	*GDP*	*AgVA*	*Credit*
-5	0.0050	-0.2824	0.0277
	(0.0200)	(1.1966)	(0.5216)
-4	0.0042	-0.5084	0.2413
	(0.0226)	(1.2264)	(0.5166)
-3	-0.0257	-0.6989	0.2377
	(0.0344)	(1.2332)	(0.6492)
-2	-0.0110	-0.5992	-1.5723
	(0.0363)	(1.2419)	(1.5837)
-1	0.0000	0.0000	0.0000
	(0.0000)	(0.0000)	(0.0000)
$+0$	0.0476	-2.7465^{*}	-0.9596
	(0.0406)	(1.4416)	(1.6910)
$+1$	0.0777^{*}	-2.8753^{*}	-1.7607
	(0.0439)	(1.7155)	(1.5424)
$+2$	0.1086^{**}	-4.5102^{**}	-0.6927
	(0.0490)	(1.8370)	(1.6272)
$+3$	0.1350^{***}	-4.7163^{**}	-1.9108
	(0.0500)	(1.8466)	(1.7133)
$+4$	0.1537^{***}	-4.2191^{**}	-3.0899^{*}
	(0.0491)	(1.7602)	(1.7767)
$+5$	0.1589^{***}	-4.5372^{***}	-4.2470^{**}
	(0.0525)	(1.6943)	(1.9098)
Pre-trend F-test p	0.546	0.946	0.735
N (country-years)	735	686	648
Countries (treated / never-treated)		22 / 12	
Country FE, Year FE		Yes	
Clustering		Country	

Notes: This table reports the full set of event-time coefficients from the Gardner (2022) two-stage difference-in-differences estimator summarized in Table 3. Each column corresponds to a different country-level outcome. k denotes years relative to mobile money launch; $k = -1$ is the omitted reference period. The first stage estimates unit and time fixed effects using only not-yet-treated and never-treated observations; the second stage regresses residualized outcomes on event-time indicators. The pre-trend F-test p-value tests the joint null that all pre-treatment coefficients ($k = -5, \ldots, -2$) are zero. Standard errors (in parentheses) are clustered at the country level. $^{***}p < 0.01$, $^{**}p < 0.05$, $^{*}p < 0.10$.

Table 5: The Effect of Drought on Vegetation

	(1)	(2)	(3)	(4)	(5)
Drought severity	−0.0365***	−0.0332***	−0.0321***	−0.0320***	−0.0323***
	(0.0083)	(0.0087)	(0.0084)	(0.0085)	(0.0085)
Drought (lagged)	0.0115*	0.0133*	0.0129*	0.0130*	0.0131*
	(0.0067)	(0.0068)	(0.0072)	(0.0072)	(0.0072)
Extreme heat		−0.0129**	−0.0128**	−0.0128**	−0.0131**
		(0.0064)	(0.0064)	(0.0064)	(0.0064)
Rainfall deficit			−0.0027	−0.0028	−0.0034
			(0.0075)	(0.0077)	(0.0075)
Conflict				−0.0046	−0.0044
				(0.0114)	(0.0113)
Radiation excess					0.0024
					(0.0085)
N	2,644	2,644	2,644	2,644	2,644
R^2 (within)	0.0132	0.0155	0.0156	0.0157	0.0157
City FE, Year FE	Yes	Yes	Yes	Yes	Yes
Clusters (country)	34	34	34	34	34

Notes: Dependent variable: $\ln(1+\text{veg share})_{i,t}$. This table estimates the direct effect of drought on vegetation without the mobile money interaction to establish that drought causes vegetation loss in the sample. Drought severity is the continuous negative soil moisture deficit anomaly from MERRA-2, standardized to city-specific means and standard deviations (equation 3). A coefficient of −0.032 implies that a one-standard-deviation soil moisture deficit reduces vegetation by 3.2 percent. Controls are added progressively across columns: extreme heat anomaly (column 2), rainfall deficit anomaly (column 3), conflict incidence (column 4), and radiation excess anomaly (column 5). Standard errors (in parentheses) are clustered at the country level. $^{***}p < 0.01$, $^{**}p < 0.05$, $^{*}p < 0.10$.

Table 6: Mobile Money and Drought Attenuation

	(1)	(2)	(3)	(4)	(5)
Drought severity	−0.0420***	−0.0389***	−0.0377***	−0.0375***	−0.0381***
	(0.0099)	(0.0102)	(0.0102)	(0.0102)	(0.0103)
Drought (lagged)	0.0134*	0.0153**	0.0148**	0.0148**	0.0150**
	(0.0071)	(0.0071)	(0.0074)	(0.0074)	(0.0074)
Mobile money	0.0081	0.0073	0.0072	0.0071	0.0074
	(0.0171)	(0.0170)	(0.0170)	(0.0169)	(0.0169)
Drought × Mobile Money	0.0319**	0.0335**	0.0340**	0.0341**	0.0346**
	(0.0158)	(0.0162)	(0.0160)	(0.0160)	(0.0160)
Extreme heat		−0.0132**	−0.0130**	−0.0131**	−0.0136**
		(0.0064)	(0.0064)	(0.0065)	(0.0064)
Rainfall deficit			−0.0035	−0.0037	−0.0046
			(0.0075)	(0.0076)	(0.0075)
Conflict				−0.0043	−0.0040
				(0.0114)	(0.0113)
Radiation excess					0.0038
					(0.0083)
N	2,644	2,644	2,644	2,644	2,644
R^2 (within)	0.0157	0.0180	0.0182	0.0183	0.0184
City FE, Year FE	Yes	Yes	Yes	Yes	Yes
Clusters	Country ($n = 34$)				

Notes: Dependent variable: $\ln(1+\text{veg share})_{i,t}$. Each column estimates equation (6) with progressively richer controls. Drought severity is the continuous negative soil moisture deficit anomaly (equation 3). Drought (lagged) is the one-year lag of drought severity, included to control for natural vegetation rebound dynamics. Mobile Money equals one in all years at or after the first mobile money launch in the country. A positive coefficient on Drought × Mobile Money indicates that mobile money attenuates drought-induced vegetation loss. Additional controls are added progressively: extreme heat anomaly (column 2), rainfall deficit anomaly (column 3), conflict incidence (column 4), and radiation excess anomaly (column 5). Standard errors (in parentheses) are clustered at the country level. $^{***}p < 0.01$, $^{**}p < 0.05$, $^{*}p < 0.10$.

Table 7: Alternative Climate Shock Definitions

	(A) Continuous drought	(B) Weighted stress index	(C) Persistent drought	(D) Binary onset (1σ)	(E) Compound drought-rain
Climate shock	-0.0381^{***}	-0.0705^{***}	-0.0357^{***}	-0.0374^{**}	-0.0321^{*}
	(0.0103)	(0.0192)	(0.0097)	(0.0186)	(0.0169)
Shock × Mobile Money	0.0346^{**}	0.0422^{*}	0.0244^{*}	0.0385	0.0599^{*}
	(0.0160)	(0.0253)	(0.0141)	(0.0253)	(0.0338)
N	2,644	2,644	2,644	2,644	2,644
R^2 (within)	0.0184	0.0183	0.0179	0.0110	0.0103
Clusters (country)	34	34	34	34	34
Heat, Conflict controls	Yes	Yes	Yes	Yes	Yes
City FE, Year FE	Yes	Yes	Yes	Yes	Yes

Notes: Dependent variable: $\ln(1+\text{veg share})_{i,t}$. Each column re-estimates the panel regression from Table 6 using a different definition of the climate shock variable. (A) Continuous soil moisture deficit anomaly (baseline). (B) Weighted climate stress index combining soil moisture deficit (50%), heat (25%), and rainfall deficit (15%), and radiation (10%). (C) Persistent drought: current deficit plus half of the prior-year deficit. (D) Binary drought onset: equals one when the soil moisture deficit exceeds one standard deviation following two consecutive non-drought years. (E) Compound drought-rain: equals one when both soil moisture and rainfall deficits simultaneously exceed one standard deviation. All specifications include the full set of controls (extreme heat, rainfall deficit, conflict, radiation excess) and the mobile money main effect, with city and year fixed effects. Standard errors (in parentheses) are clustered at the country level. $^{***}p < 0.01$, $^{**}p < 0.05$, $^{*}p < 0.10$.

Table 8: Cross-Hazard Placebo: Does Mobile Money Buffer All Climate Shocks?

	(1) Drought	(2) Heat	(3) Rainfall deficit
Climate shock	−0.0381***	−0.0152**	0.0141**
	(0.0103)	(0.0073)	(0.0071)
Shock × Mobile Money	0.0346**	0.0069	0.0084
	(0.0160)	(0.0135)	(0.0164)
Extreme heat	−0.0136**		−0.0314***
	(0.0064)		(0.0086)
Drought severity		−0.0313***	0.0190
		(0.0086)	(0.0139)
Rainfall deficit	0.0150**	0.0141**	
	(0.0074)	(0.0072)	
Conflict	−0.0011	−0.0009	−0.0023
	(0.0019)	(0.0019)	(0.0022)
N	2,644	2,644	2,644
R^2 (within)	0.0184	0.0167	0.0175
Clusters (country)	34	34	34
City FE, Year FE		Yes	

Notes: Dependent variable: $\ln(1 + \text{veg share})_{i,t}$. Each column estimates a separate panel regression with a different climate shock interacted with mobile money availability. All specifications include the other two climate shocks and conflict as controls, with city and year fixed effects. If mobile money specifically buffers drought (through enabling transfers and savings), the interaction should be significant for drought but not for heat, which causes biophysical damage that financial transfers cannot reverse. Standard errors (in parentheses) are clustered at the country level. $^{***}p < 0.01$, $^{**}p < 0.05$, $^{*}p < 0.10$.

Table 9: Heterogeneity: Drought × MM by Subsample

	High			Low			
Dimension	$\hat{\beta}$	SE	N	$\hat{\beta}$	SE	N	p(diff)
Aridity (semi-arid)	0.0320**	(0.0160)	1,321	0.0331*	(0.0200)	1,323	0.967
Private credit / GDP	0.0438**	(0.0221)	1,149	0.0323	(0.0220)	1,495	0.711
Financial development	0.0253	(0.0224)	1,264	0.0364	(0.0261)	1,380	0.748
Bank branch density	0.0327**	(0.0148)	1,161	0.0145	(0.0249)	1,483	0.530
Common law (English)	0.0303*	(0.0179)	451	0.0362**	(0.0165)	2,113	0.809
Civil law (French)	0.0388**	(0.0179)	1,868	0.0522***	(0.0088)	696	0.504
Mobile money penetration	0.0098	(0.0286)	871	0.0354	(0.0229)	1,773	0.484
Banking stability	0.0227	(0.0235)	1,107	0.0406*	(0.0218)	1,537	0.576
Conflict history	0.0244	(0.0166)	2,283	0.0907	(0.0593)	361	0.282
Controls	Heat, Conflict						
City FE, Year FE	Yes						

Notes: This table examines whether the drought attenuation effect of mobile money varies across observable dimensions. For each row, the sample is split at the country-level median of the indicated variable, and the baseline panel regression (equation 6) is estimated separately on each subsample. "High" and "Low" refer to above- and below-median groups. The final column reports the p-value from a two-sided test of the null that the High and Low coefficients are equal, computed as $z = (\hat{\beta}_H - \hat{\beta}_L)/\sqrt{\text{SE}_H^2 + \text{SE}_L^2}$, which is conservative because it ignores any positive covariance between subsample estimators. Aridity is classified by below-median city average rainfall. Private credit/GDP, financial development, bank branch density, mobile penetration, and banking stability are split at the country-level median using data from the World Development Indicators and Global Financial Development Database. Common law and civil law are binary indicators following La Porta et al. (1998) legal origin classifications. Conflict history indicates countries whose `conflict_any` variable equals one in at least one sample year. All specifications include city and year fixed effects with heat and conflict controls. Standard errors (in parentheses) are clustered at the country level. $^{***}p < 0.01$, $^{**}p < 0.05$, $^{*}p < 0.10$.

Table 10: Encompassing Specification: Mobile Money vs. Bank Branches vs. Private Credit

	$\ln(1 + \text{veg share})_{i,t}$
Drought severity	-0.0496^{***}
	(0.0119)
Drought × Mobile Money	0.0391^{**}
	(0.0158)
Drought × Bank Branches	-0.0017
	(0.0237)
Drought × Private Credit	0.0227
	(0.0249)
Extreme heat	-0.0132^{**}
	(0.0064)
Conflict	-0.0039
	(0.0109)
N	2,644
R^2 (within)	0.0195
Clusters (country)	34
City FE, Year FE	Yes

Notes: Dependent variable: $\ln(1 + \text{veg share})_{i,t}$. This table reports an encompassing specification that simultaneously includes mobile money, bank branch density, and private credit to GDP, each interacted with drought severity. "Bank Branches" and "Private Credit" are above-median binary indicators constructed from the World Bank GFDD. If the drought attenuation result reflects general financial depth rather than mobile money specifically, bank branches and private credit should also be significant. Standard errors (in parentheses) are clustered at the country level. $^{***}p < 0.01$, $^{**}p < 0.05$, $^{*}p < 0.10$.

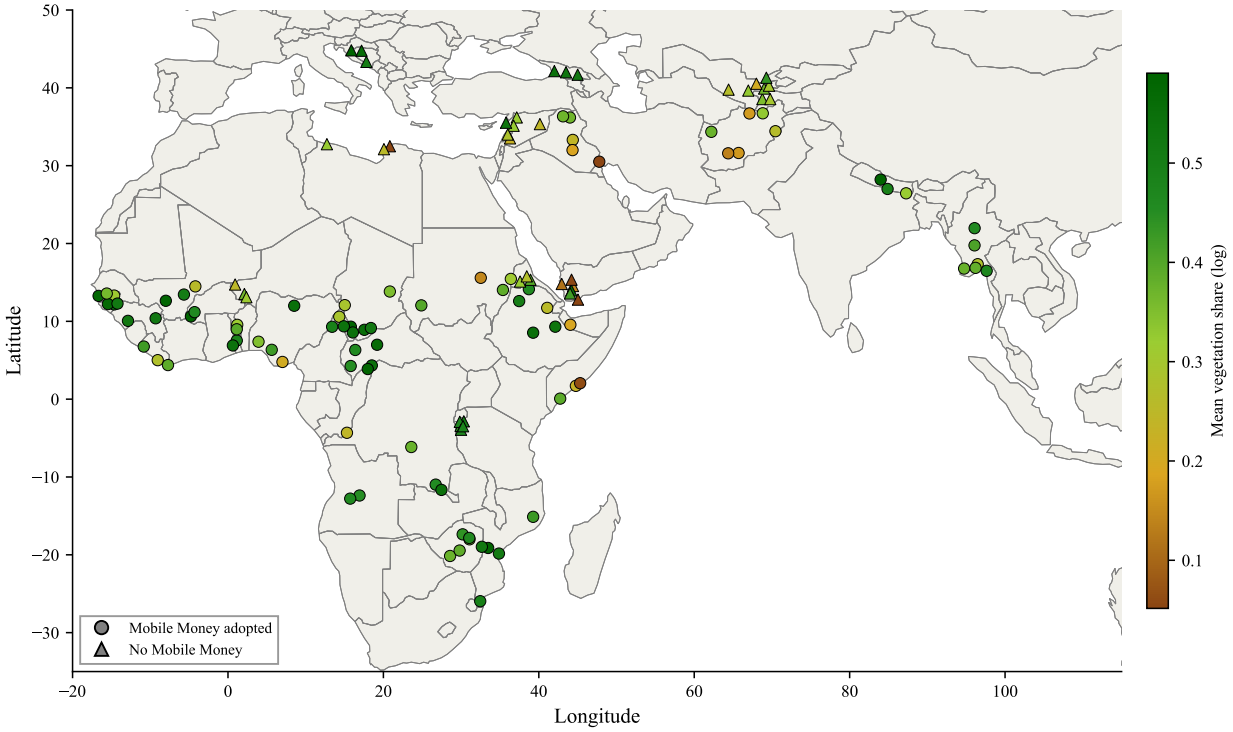


Figure 1: Spatial distribution of the 132 cities in the sample, drawn from 34 countries classified as Fragile and Conflict-Affected States by the World Bank. Countries are shaded in light grey. Circles denote cities in countries that adopt mobile money during the sample period; triangles denote cities in non-adopter countries. Marker color indicates mean log vegetation share (darker green = higher vegetation). For most countries, the two to five largest non-capital cities with identifiable farmland are included. Of the 132 cities, 81 are in Sub-Saharan Africa (22 countries); the remaining 51 span the Middle East, South and Central Asia, Southeast Asia, Europe, and South America (12 countries).

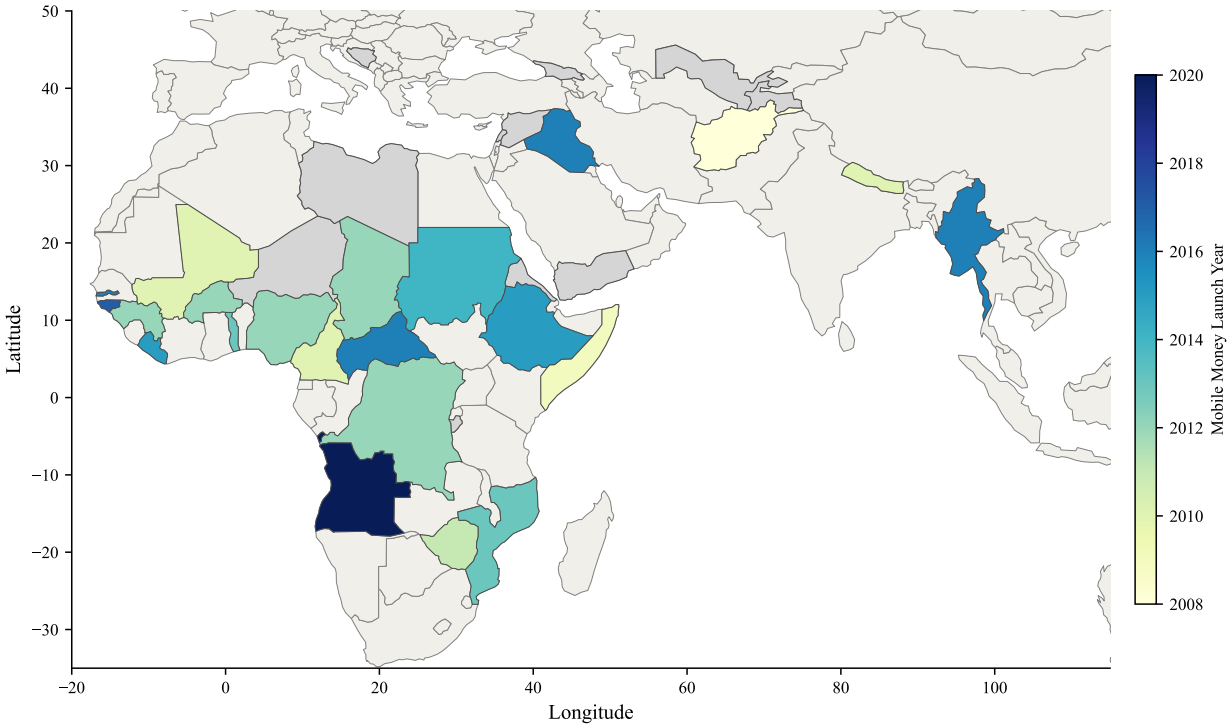


Figure 2: Year of first mobile money service launch by country, drawn from the GSMA Mobile Money Deployment Tracker. Darker shading indicates earlier adoption. Of the 34 sample countries, 22 adopt mobile money during the sample period (2000–2021); the remaining 12 (unshaded) serve as never-treated controls. Afghanistan (2008) and Somalia (2009) were the earliest adopters in the sample, with adoption accelerating across Sub-Saharan Africa through the 2010s.

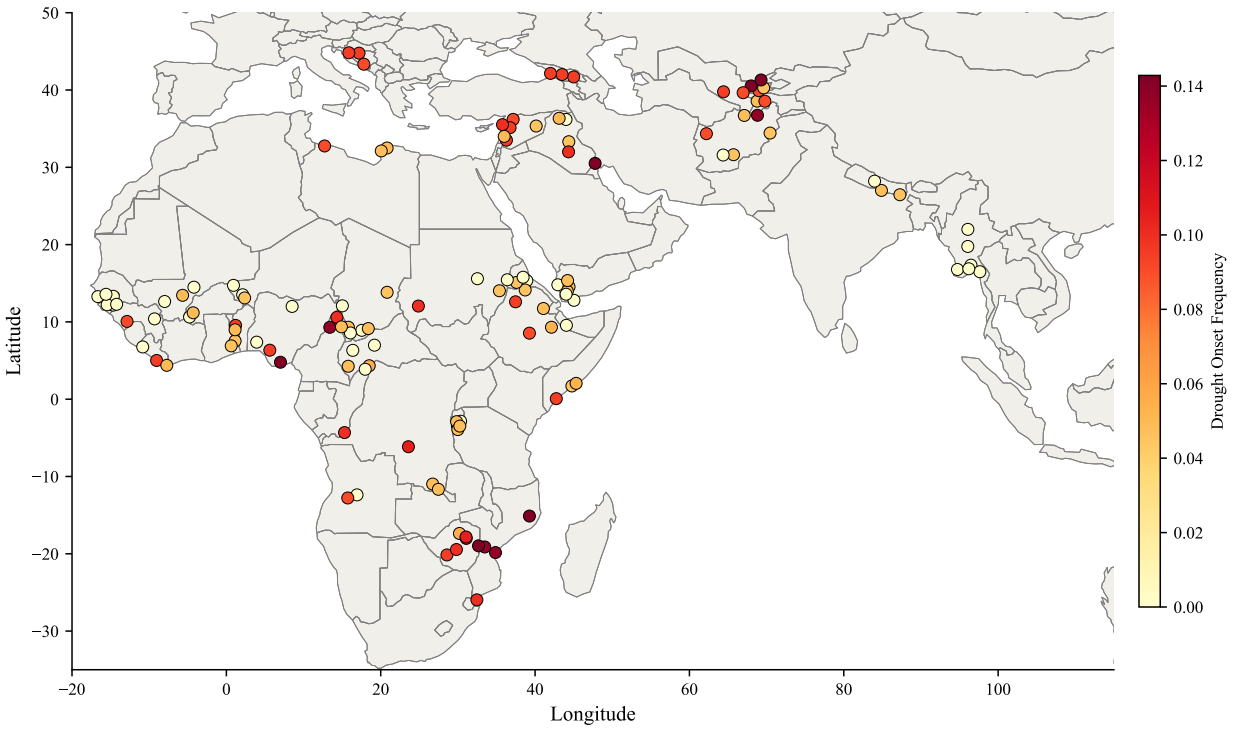


Figure 3: Drought frequency by city, measured as the share of city-year observations in which the standardized soil moisture anomaly exceeds one standard deviation below the city-specific mean. Each point represents one of the 132 sample cities, colored by drought onset frequency (darker = more frequent). Soil moisture data are from the MERRA-2 reanalysis ($0.5° \times 0.625°$ resolution). Cities in the Sahel and Horn of Africa experience the highest drought frequency, while coastal West African and Southeast Asian cities are less frequently affected.

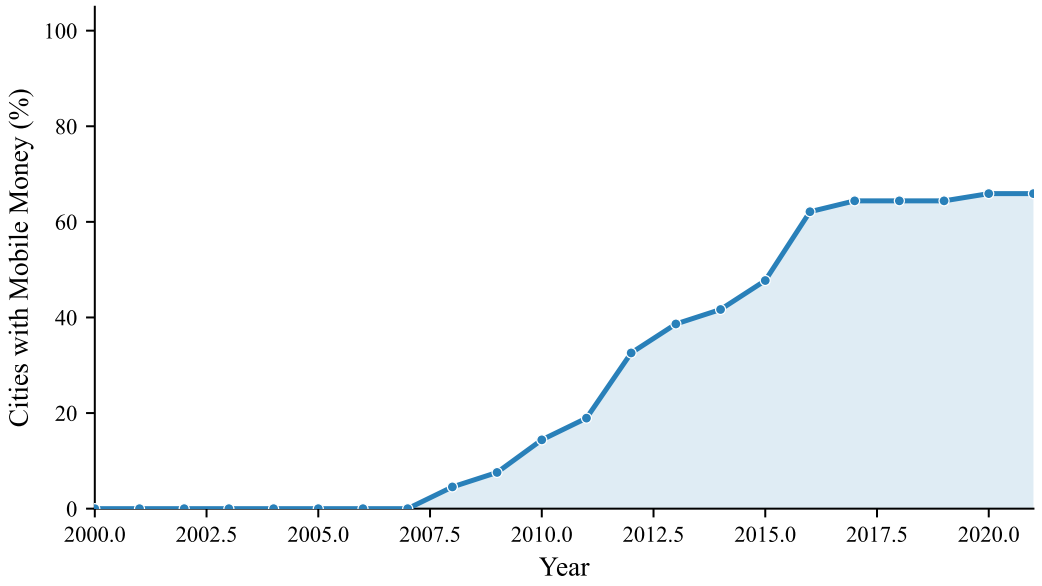


Figure 4: Cumulative share of sample cities located in countries with an active mobile money service, 2000–2021. The vertical axis measures the percentage of the 132 sample cities in countries where mobile money has launched, using a fixed denominator of 132 cities. Adoption is coded at the country level using the GSMA launch year. The figure shows a sharp acceleration after 2010, reaching approximately 48 percent by 2015 and 62 percent by 2016.

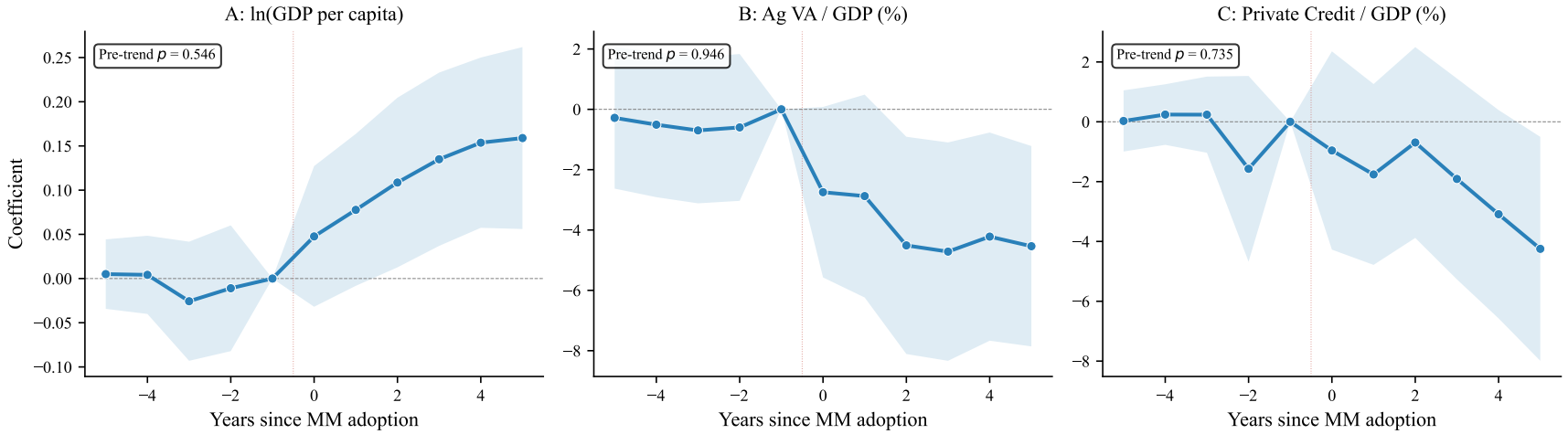


Figure 5: Gardner (2022) two-stage difference-in-differences event study estimates around mobile money adoption, for three country-level outcomes. Panel A plots coefficients for log GDP per capita; Panel B for agricultural value added as a share of GDP; Panel C for domestic credit to the private sector as a share of GDP. The horizontal axis measures years relative to the country's mobile money launch year ($k = 0$); $k = -1$ is the omitted reference period. The vertical dashed red line marks the adoption year. Point estimates are shown with circles connected by solid lines; shaded bands represent 95% confidence intervals based on country-clustered standard errors. Flat pre-period coefficients support the parallel trends assumption; post-adoption divergence indicates treatment effects.

Internet Appendix

A. Additional Tables

Table A.1: Robustness to Country × Year Fixed Effects

	(1) Year FE	(2) Country×Year FE
Drought severity	−0.0375***	−0.0307**
	(0.0102)	(0.0130)
Drought × MM	+0.0341**	+0.0066
	(0.0160)	(0.0231)
Heat stress	−0.0131**	−0.0196***
	(0.0065)	(0.0075)
Rainfall deficit	−0.0037	−0.0094
	(0.0076)	(0.0091)
Conflict	−0.0043	−0.0020
	(0.0114)	(0.0131)
N	2,644	2,644
R^2	0.018	0.012
Clusters	34	34

Notes: This table examines whether the drought attenuation result is robust to replacing year fixed effects with country×year fixed effects, which absorb all country-level time-varying confounders (e.g., macroeconomic policy, commodity price exposure, regulatory changes). Column (1) reproduces the baseline specification from Table 6 column (4) with city and year fixed effects. Column (2) replaces year fixed effects with country×year interactions. With approximately four cities per country, these stringent fixed effects absorb most identifying variation, which accounts for the loss of significance in the interaction term. The dependent variable is ln(1 + veg share). Standard errors (in parentheses) are clustered at the country level. $^{***}p < 0.01$, $^{**}p < 0.05$, $^{*}p < 0.10$.

Table A.2: Drought Attenuation by Mobile Money: Multiple Outcomes

	Veg share (city)	ln(GDP p.c.)	Ag VA/GDP	ln(Cereal)
Drought severity	−0.0399***	−0.0570	1.6601	−0.0212
	(0.0103)	(0.0520)	(1.0550)	(0.0321)
Drought × MM	0.0370**	0.1267	−0.6416	−0.0400
	(0.0175)	(0.0924)	(1.8644)	(0.0679)
N	2,644	732	683	745
R^2	0.018	0.017	0.021	0.016
Clusters	34	34	33	34
Controls		Heat, Conflict		
City FE, Year FE		Yes		

Notes: This table estimates the baseline panel regression (equation 6) using four different dependent variables. Column (1) uses city-level ln(1 + veg share), the main outcome in the paper. Columns (2)–(4) use country-level outcomes from the World Development Indicators: log GDP per capita, agricultural value added as a share of GDP, and log cereal yield (kg per hectare). The city-level vegetation share measure, observed for 132 cities over 21 years, provides substantially more statistical power than the country-level aggregates (32 countries over ∼22 years). This power advantage explains why the attenuation effect is detectable only in the vegetation share specification. Standard errors (in parentheses) are clustered at the country level. $^{***}p < 0.01$, $^{**}p < 0.05$, $^{*}p < 0.10$.

Table A.3: Alternative Inference: Standard Errors on Drought × Mobile Money

	(1)	(2)	(3)	(4)	(5)
Drought × MM (coef.)	+0.0319**	+0.0335**	+0.0340**	+0.0341**	+0.0346**
Country-clustered	(0.0158)	(0.0162)	(0.0160)	(0.0160)	(0.0160)
Driscoll-Kraay	(0.0157)	(0.0154)	(0.0154)	(0.0154)	(0.0154)
Conley Bartlett 500km	(0.0151)	(0.0152)	(0.0150)	(0.0151)	(0.0151)
Conley Bartlett 1000km	(0.0152)	(0.0152)	(0.0150)	(0.0150)	(0.0151)
Conley Bartlett 1500km	(0.0148)	(0.0149)	(0.0146)	(0.0147)	(0.0147)
Ratio: Driscoll-Kraay / Clustered	0.99×	0.95×	0.96×	0.96×	0.96×
Ratio: Conley Bartlett 500km / Clustered	0.96×	0.94×	0.94×	0.94×	0.94×
Ratio: Conley Bartlett 1000km / Clustered	0.96×	0.94×	0.94×	0.94×	0.94×
Ratio: Conley Bartlett 1500km / Clustered	0.94×	0.92×	0.92×	0.91×	0.92×

Notes: This table reports standard errors for the Drought × Mobile Money coefficient from Table 6 under alternative inference procedures. Row 1 reproduces the baseline country-clustered standard errors. Row 2 reports Driscoll-Kraay (1998) standard errors, which are robust to arbitrary cross-sectional and temporal dependence. Rows 3–5 report Conley (1999) spatial HAC standard errors with Bartlett kernels at 500, 1,000, and 1,500 km cutoffs. Ratios below 1 indicate tighter inference than clustering; ratios above 1 indicate wider inference. Significance: *** $p < 0.01$, ** $p < 0.05$, * $p < 0.10$.

Table A.4: Variable Descriptions

Variable	Description
country	Name of the country where the observation was recorded.
city	Name of the city within the country.
year	Year of the observation.
total	Total area calculated from ArcGIS histogram: .sum() $\times$ 0.0009.
vegetation	Vegetation area where index ≥ 0.2, calculated as count $\times$ 0.0009 from histogram.
ratio	Ratio of vegetation to total.
type_of_violence	Type of conflict event from the conflict dataset.
best	Number of conflict-related deaths in the city; missing values replaced with zero.
best_country	Total conflict-related deaths aggregated at the country–year level.
m2tmnxslv_5_12_4_t2m	Yearly average 2-meter air temperature (MERRA-2 monthly, city level).
m2smnxslv_5_12_4_t2mmax	Yearly average daily max 2-meter air temperature (MERRA-2 monthly, city level).
m2smnxslv_5_12_4_t2mmin	Yearly average daily min 2-meter air temperature (MERRA-2 monthly, city level).
gpm_3imergm_07_precipitation	Yearly average precipitation estimate (IMERG Final Run, city level).

continued next page

Variable	Description
m2tmnxlnd_5_12_4_rzmc	Yearly average root zone soil moisture content (MERRA-2 monthly, city level).
m2tmnxflx_5_12_4_speed	Yearly average surface wind speed (MERRA-2 monthly, city level).
m2tmnxrad_5_12_4_swgnt	Yearly average net downward shortwave flux (MERRA-2 monthly, city level).
TotalAssets_sum_both to NPLRatio_mean_supranational	Aggregated financial metrics from BankFocus database for banks operating at different levels (national, supranational, and both), including sums and means of total assets, loans, equity, income, reserves, ROAA, cost-to-income ratio, Tier 1 ratio, and NPL ratio.
Account (% age 15+)	Percentage of population (15+) with any financial account (FinDex).
Financial institution account (% age 15+)	Percentage with account at a financial institution (FinDex).
Mobile money account (% age 15+)	Percentage with a mobile money account (FinDex).
Made or received a digital payment (% age 15+)	Percentage who made/received digital payments (FinDex).
Saved at a financial institution (% age 15+)	Percentage who saved money at a financial institution (FinDex).

continued next page

Variable	Description
Borrowed any money from a formal financial institution or using a mobile money account (% age 15+)	Percentage who borrowed from formal institutions or via mobile money (FinDex).
Account, female (% age 15+)	Percentage of females with financial accounts (FinDex).
Account, male (% age 15+)	Percentage of males with financial accounts (FinDex).
popu_census	City-level population from census year.
popu_census_ipolated	Interpolated census population for years between official census dates.
census	Source indicator for census-based population values.
popu_projected	Officially projected population values for city–year.
popu_projected_ipolated	Interpolated projections between available years.
access_bankaccounts	Number of depositors with commercial banks per 1,000 adults.
access_bankbranches	Number of commercial bank branches per 100,000 adults.
access_valueadded	Value of all traded shares outside of the largest ten traded companies as a share of total value of all traded shares in a stock market exchange.

continued next page

Variable	Description
access_marketcapitalizati	Value of listed shares outside of the largest ten largest companies to total value of all listed shares.
depth_privatecredit	The financial resources provided to the private sector by domestic money banks as a share of GDP. Domestic money banks comprise commercial banks and other financial institutions that accept transferable deposits, such as demand deposits.
depth_liquid_liabili	Ratio of liquid liabilities to GDP. Liquid liabilities are also known as broad money, or M3. They are the sum of currency and deposits in the central bank (M0), plus transferable deposits and electronic currency (M1), plus time and savings deposits, foreign currency transferable deposits, certificates of deposit, and securities repurchase agreements (M2), plus travelers checks, foreign currency time deposits, commercial paper, and shares of mutual funds or market funds held by residents.
depth_privatecredit_financial	Private credit by deposit money banks and other financial institutions to GDP.
depth_stockmktcapitalizatio	Total value of all listed shares in a stock market as a percentage of GDP.
depth_domdebtsecur	Total amount of domestic private debt securities (amount outstanding) issued in domestic markets as a share of GDP. It covers data on long-term bonds and notes, commercial paper and other short-term notes.

continued next page

Variable	Description
effic_bnkrmargin	Accounting value of bank's net interest revenue as a share of its average interest-bearing (total earning) assets.
effic_bnklendingdeposit	Difference between lending rate and deposit rate. Lending rate is the rate charged by banks on loans to the private sector and deposit interest rate is the rate offered by commercial banks on three-month deposits.
effic_bnkoverheadcost	Bank overhead costs as a share of total assets, reflecting operational efficiency of banks.
effic_stockmrkturnover	Total value of shares traded during the period divided by the average market capitalization for the period.
stabi_bankZscore	It captures the probability of default of a country's commercial banking system. Z-score compares the buffer of a country's commercial banking system (capitalization and returns) with the volatility of those returns.
stabi_bnknonperformloan	Ratio of defaulting loans (payments of interest and principal past due by 90 days or more) to total gross loans (total value of loan portfolio). The loan amount recorded as nonperforming includes the gross value of the loan as recorded on the balance sheet, not just the amount that is overdue.

continued next page

Variable	Description
stabi_stockP_vola	Bank's income that has been generated by noninterest related activities as a percentage of total income (net-interest income plus noninterest income). Noninterest related income includes net gains on trading and derivatives, net gains on other securities.
legor_uk	Dummy variable equal to 1 if the country's legal origin is English (common law) and 0 otherwise. English-origin systems emphasize judicial independence, private property rights, and market-supporting legal structures.
legor_fr	Dummy variable equal to 1 if the country's legal origin is French (civil law) and 0 otherwise. French-origin systems are characterized by codified laws and greater state involvement in economic and legal regulation.
legor_ge	Dummy variable equal to 1 if the country's legal origin is German (civil law) and 0 otherwise. German-origin systems emphasize comprehensive codification, legal formalism, and structured administrative oversight.
legor_sc	Dummy variable equal to 1 if the country's legal origin is Scandinavian and 0 otherwise. Scandinavian-origin systems combine features of civil law traditions with pragmatic legal interpretation and strong welfare-state institutions.

continued next page

Variable	Description
`legor_so`	Dummy variable equal to 1 if the country's legal origin is Socialist and 0 otherwise. Socialist-origin systems are based on state ownership and central planning principles, reflecting the institutional legacies of former socialist regimes.

Table A.6: Sample Countries and Cities

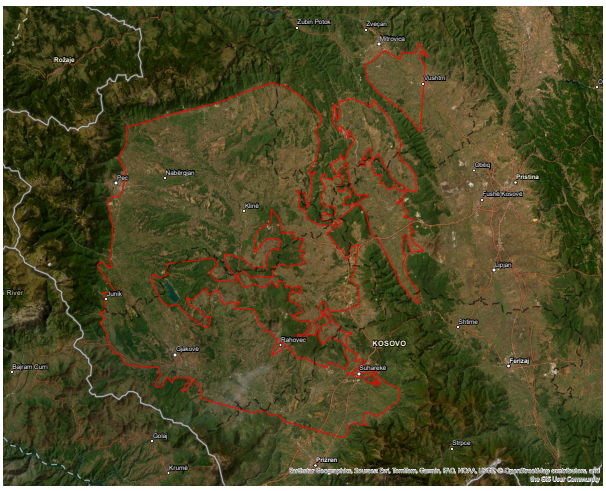
Countries	**Cities/ Towns**
Afghanistan	Herat; Jalalabad; Kandehar; Kondur; Lashgargah; Mazaresharif
Angola	Cuito; Huambo
Bosnia and Herzegovina	Banjaluca; Bihac; Mostar
Burkina Faso	Banfora; Bobo-Dioulasso
Burundi	Gitega; Muyinga; Ngozi; Rutana; Ruyigi
Cameroon	Garoua; Kousseri; Maroua
Central African Republic	Berberati; Bimbo; Bozoum; Kaga-Bandoro; Mbaiki
Chad	Abeche; Kelo; Koumra; Moundou; Pala; Sarh
Democratic Republic of Congo	Kinshasa; Likasi; Lubumbashi; Mbuji-Mayi
Eritrea	Asmara; Barentu; Keren
Ethiopia	Axum; Dubti; Gondar; Harar; Nazreth/ Adama
Gambia	Brikama; Basse; Farafenni
Georgia	East; Mid; West
Guinea	Kankan; Kindia
Guinea-Bissau	Bafata; Bissora; Gabu
Iraq	Baghdad; Basrah; Erbil; Mosul; Najaf
Lebanon	Up
Liberia	Bomi; Greenville; Harper
Libya	Al-ZÄwiyah; Benghazi; El Marg/ Al Marg
Mali	Bamako; Mopti; Segou
Mozambique	Beira; Chimoio; Matola; Nampula
Myanmar	Bago; Mandalay; Mawlamyine; Naypyidaw; Pathein; Yangon
Nepal	Biratnagar; Birgunj; Pokhara
Niger	Ayorou; Niamey; Say
Nigeria	Benin City; Ibadan; Kano; Port Harcourt
Somalia	Hargeisa; Jamaame; Marka/ Merca; Mogadishu
Sudan	Al Qadarif; Kassala; Khartoum; Nyala
Syria	Aleppo; Damascus; Deir ez-Zor; Hama
Tajikistan	Dushanbe; Istaravshan; Khujand; Kulob
Togo	Atakpame; Kara; Kpalime; Sokode
Uzbekistan	Bukhara; Mamangan; Samarkand; Tashkent
Venezuela	Cabimas; Ciudad BolÃvar; ColÃ³n; Guanare; Maturin
Yemen	Aden; Al Hudaydah; Dhamar; Ibb; Sanaa; Taizz
Zimbabwe	Bulawayo; Chinhoyi; Chitungwiza; Gweru; Harare; Mutare

B. NDVI Construction

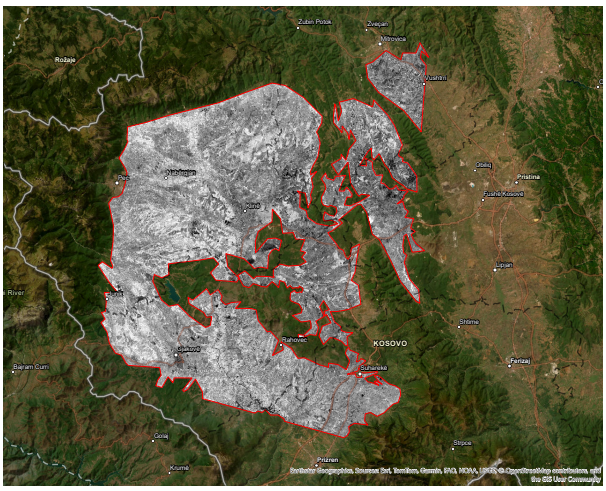


Figure A.1: Example of manually delineated farmland boundaries within a sample city. The highlighted polygons identify agricultural and peri-urban farmland areas within which NDVI is computed. Built-up areas, water bodies, and natural (non-agricultural) vegetation are excluded. This delineation is performed for each of the 132 cities in the sample; the full set of city-level maps appears in Section C of this Appendix.

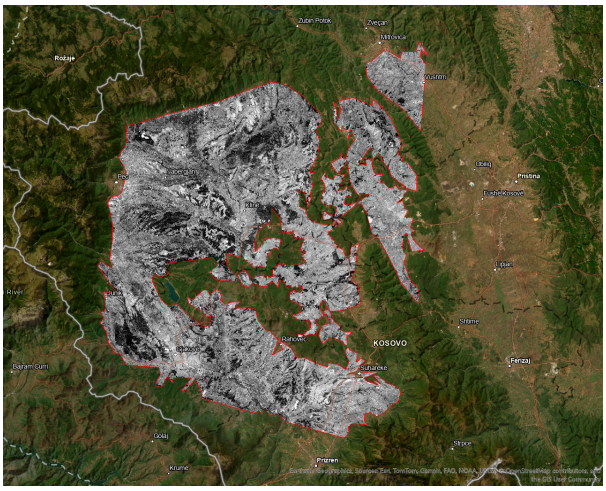
Figure A.2: Workflow for computing the Normalized Difference Vegetation Index (NDVI). Steps include delineating agricultural boundaries, extracting spectral bands, computing NDVI, and deriving pixel-based vegetation histograms. Example: Kosovo, 2022.



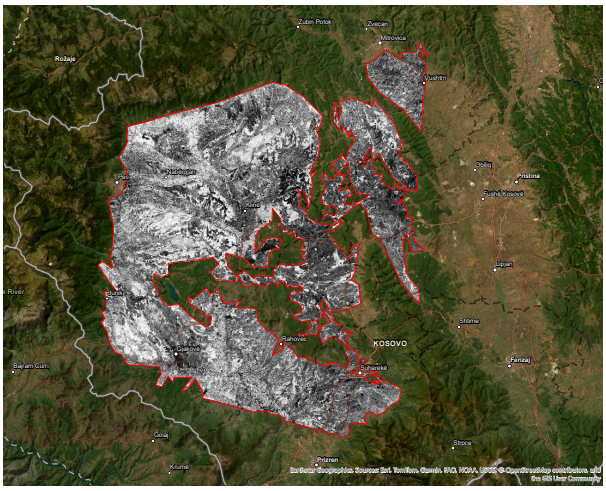
(a) Boundary delineation of farmlands.



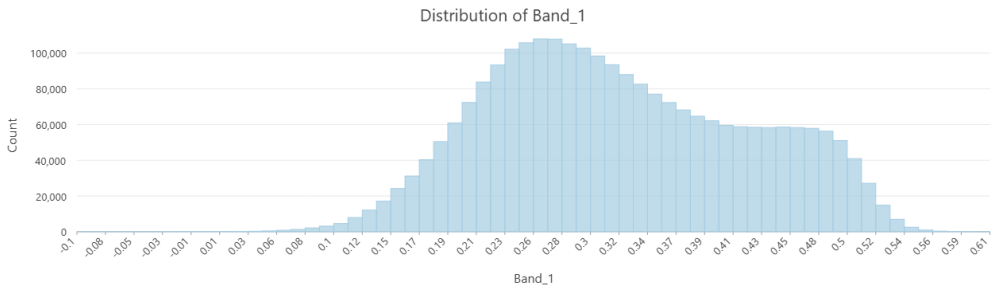
(b) Near-infrared (Band 5) raster.



(c) Red (Band 4) raster.



(d) NDVI raster computed from NIR and Red bands.

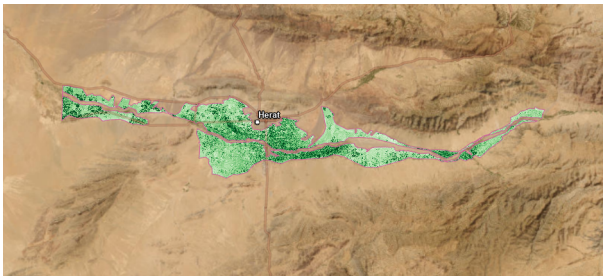


(e) NDVI histogram showing pixel intensity distribution.

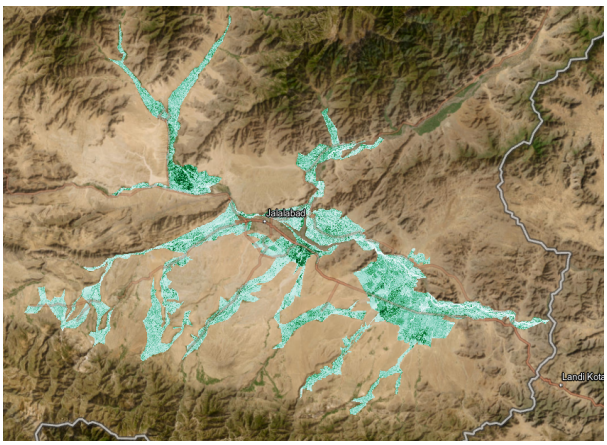
C. City-Level Satellite Images

The following pages display the delineated farmland boundaries for each city in the sample, organized by country. These boundaries define the spatial extent over which NDVI is computed.

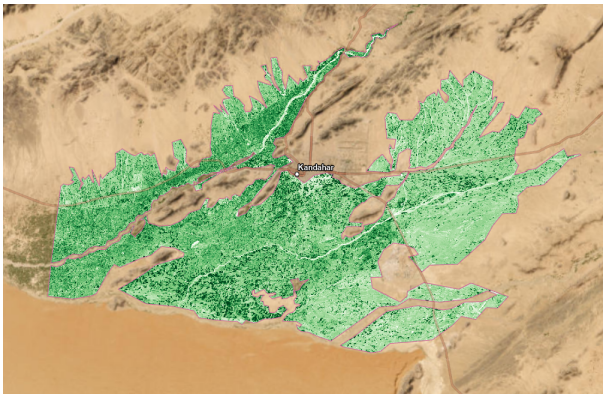
Figure A.3: Afghanistan: Delineated Farmland Areas



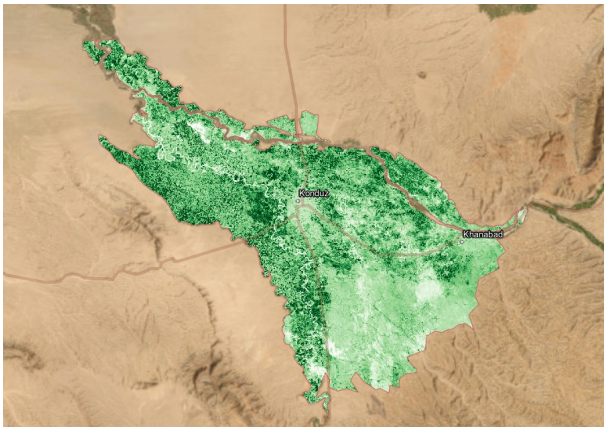
(a) Herat



(b) Jalalabad



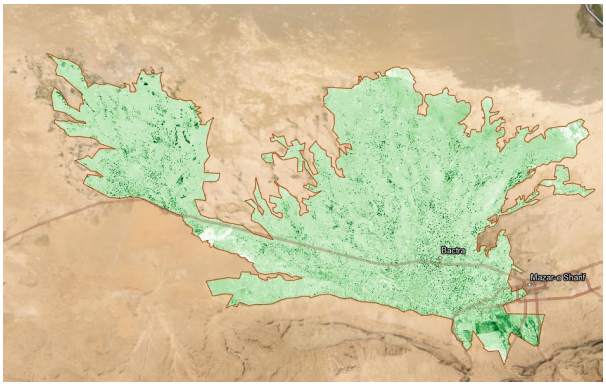
(c) Kandahar



(d) Konduz

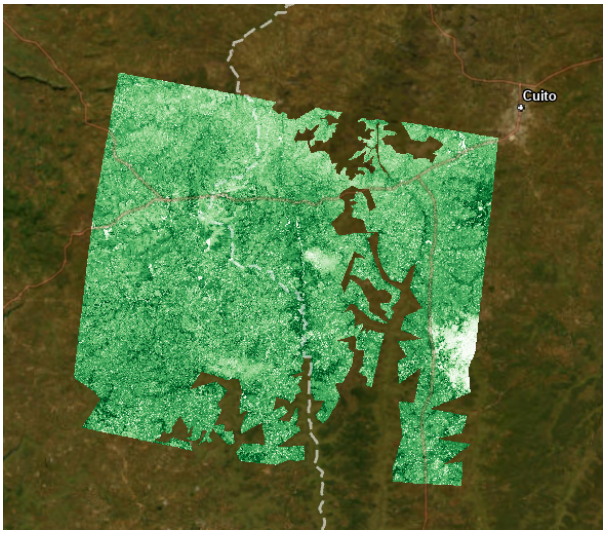


(e) Lashkar Gah

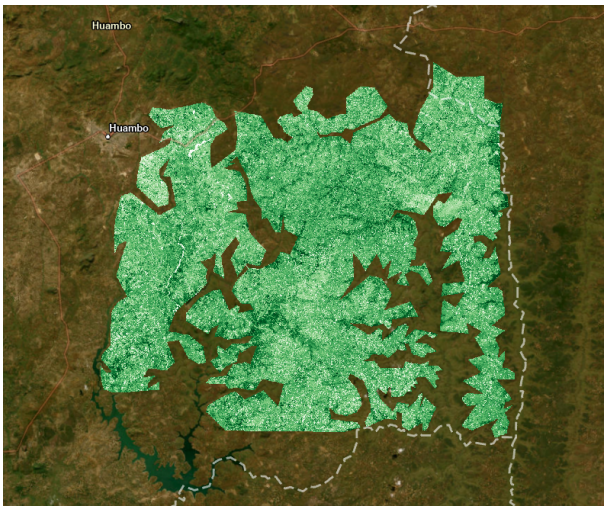


(f) Mazar-e-Sharif

Figure A.4: Angola: Delineated Farmland Areas

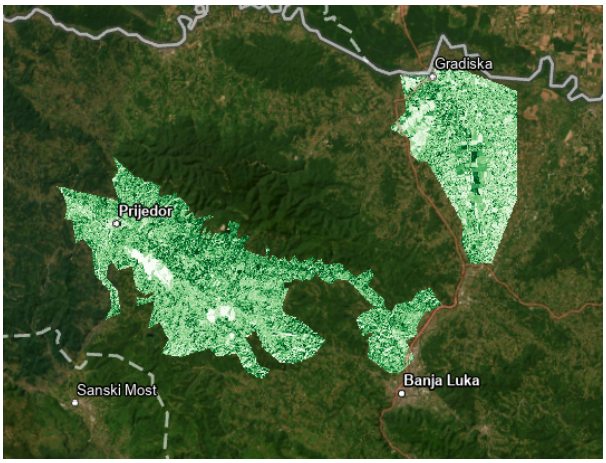


(a) Cuito

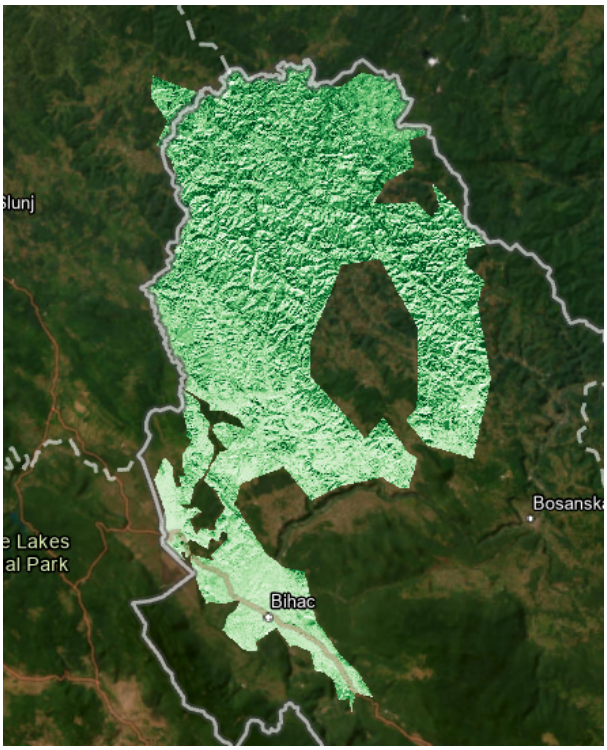


(b) Huambo

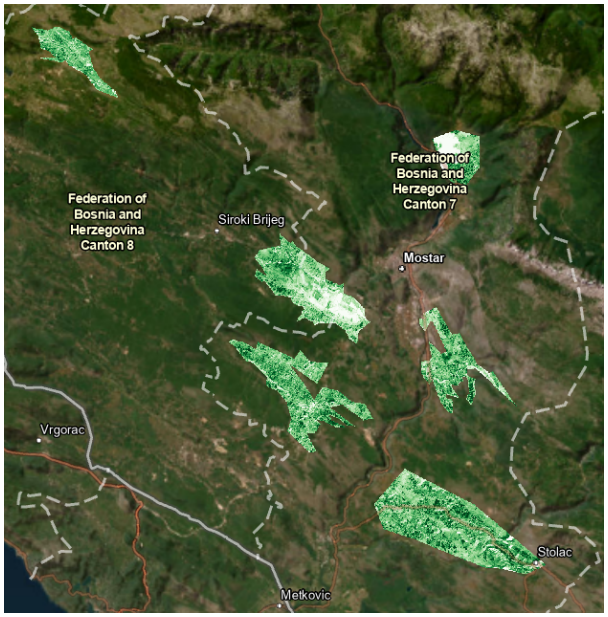
Figure A.5: Bosnia and Herzegovina: Delineated Farmland Areas



(a) Banja Luka

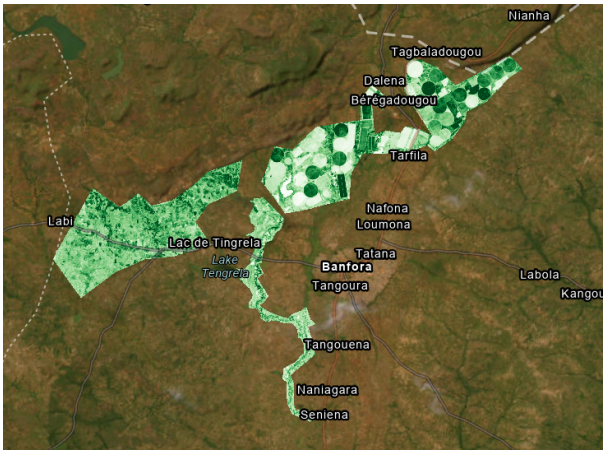


(b) Bihać

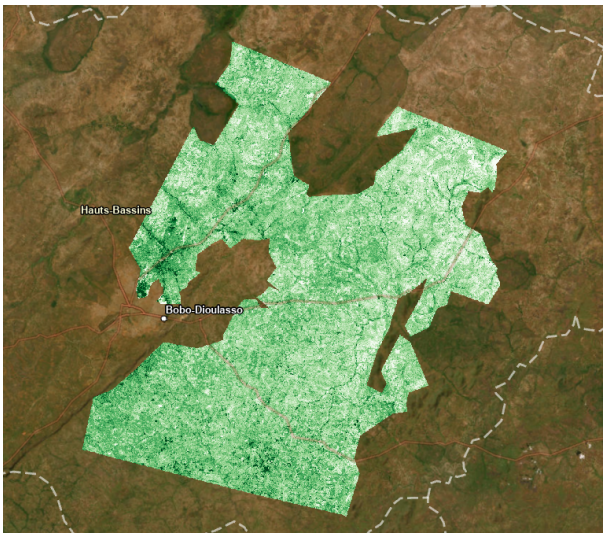


(c) Mostar

Figure A.6: Burkina Faso: Delineated Farmland Areas

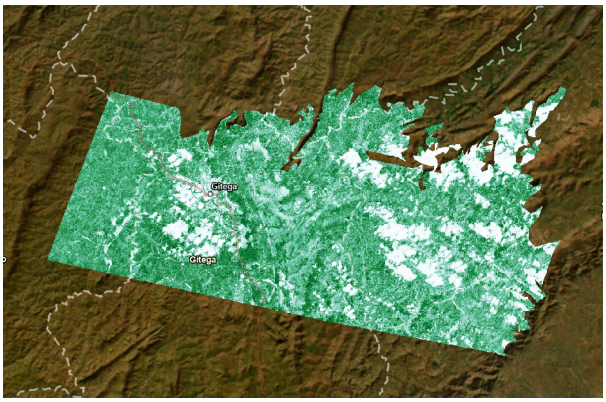


(a) Banfora

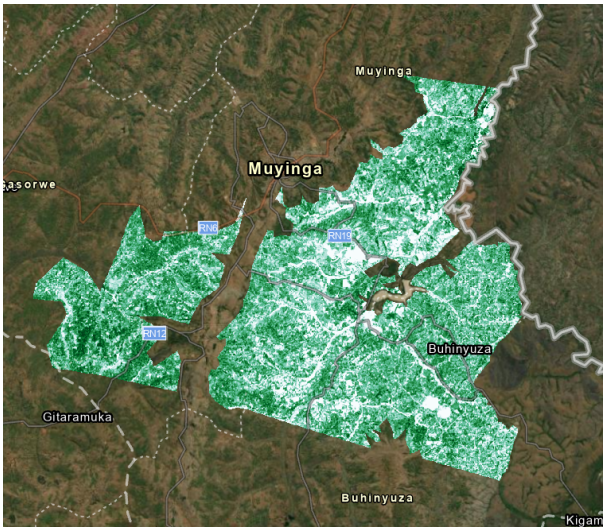


(b) Bobo-Dioulasso

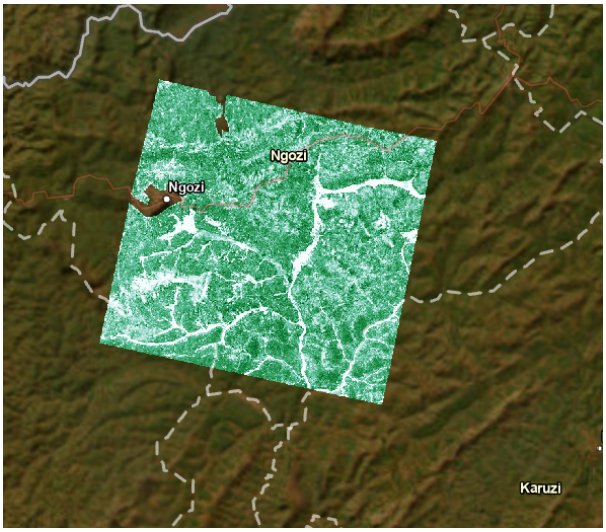
Figure A.7: Burundi: Delineated Farmland Areas



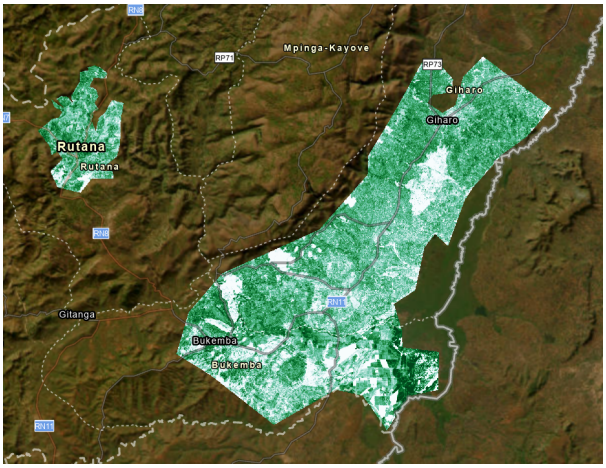
(a) Gitega



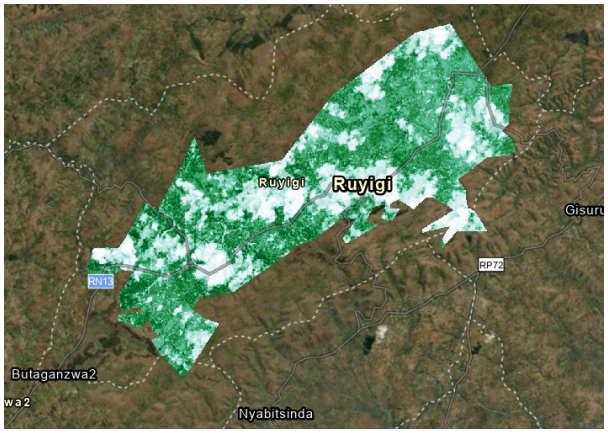
(b) Muyinga



(c) Ngozi

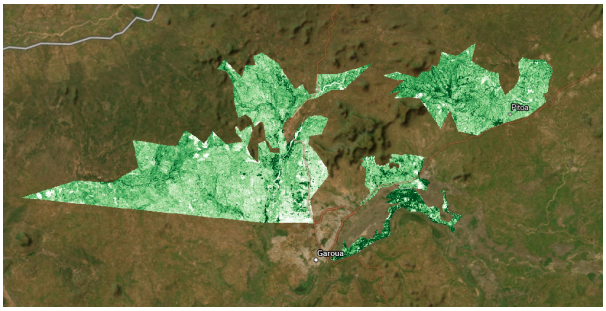


(d) Rutana

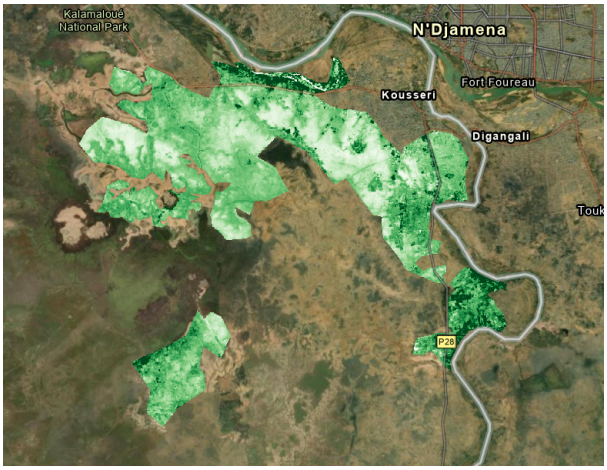


(e) Ruyigi

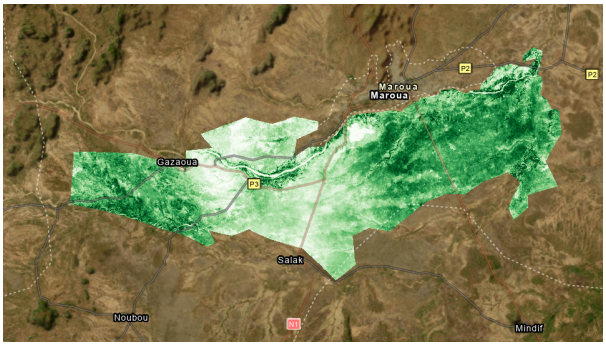
Figure A.8: Cameroon: Delineated Farmland Areas



(a) Garoua

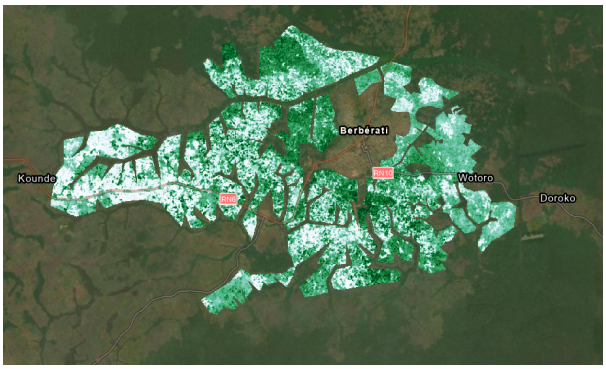


(b) Kousseri

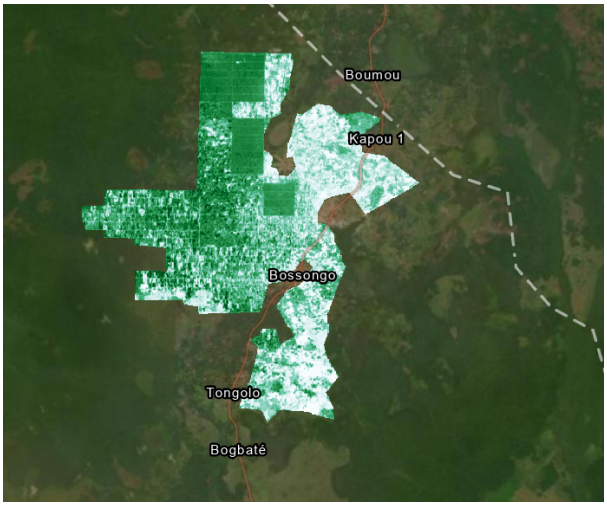


(c) Maroua

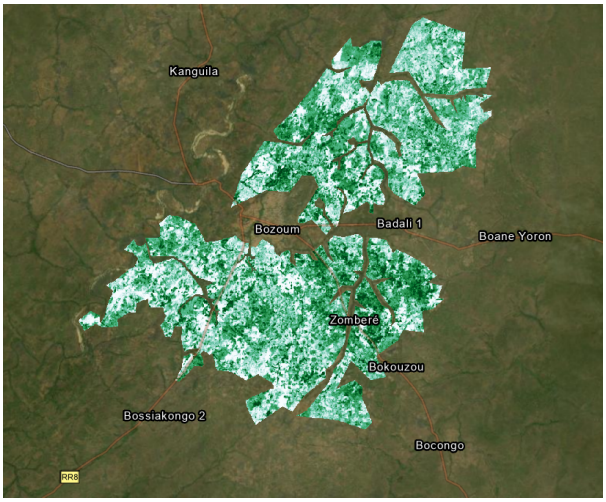
Figure A.9: Central African Republic: Delineated Farmland Areas



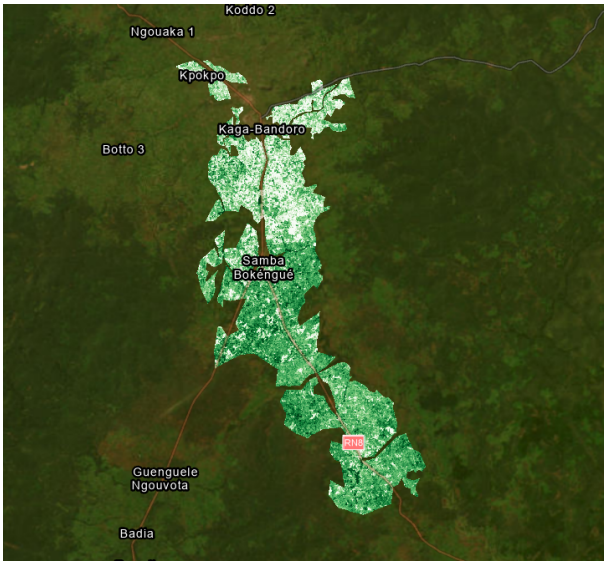
(a) Bérbérati



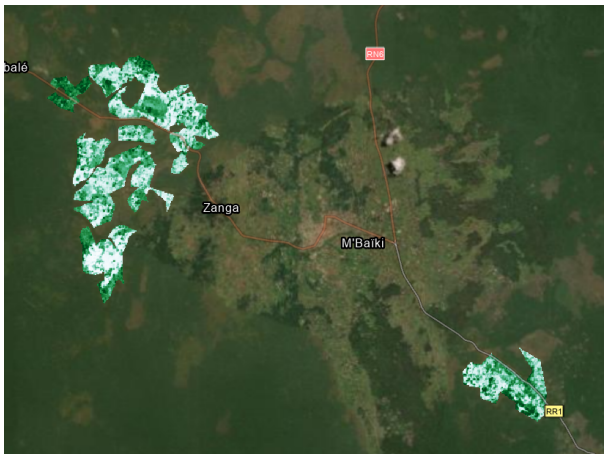
(b) Bimbo



(c) Bozoum



(d) Kaga-Bandoro

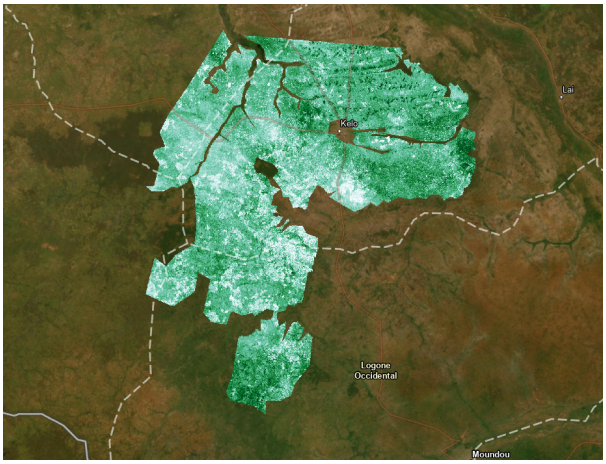


(e) M'baïki

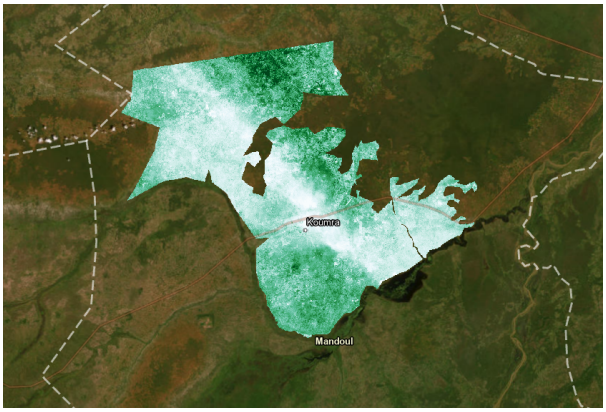
Figure A.10: Chad: Delineated Farmland Areas



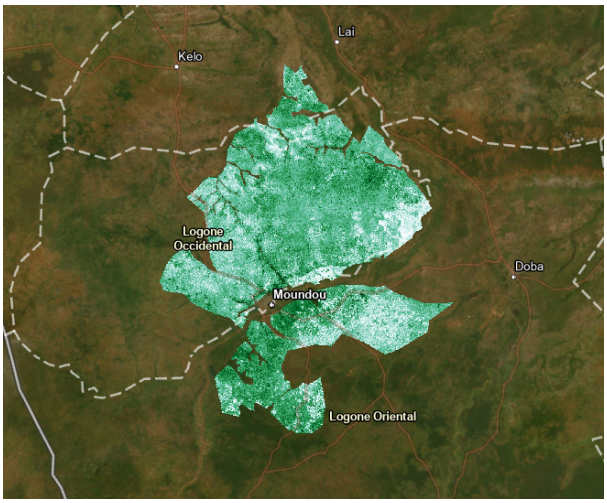
(a) Abéché



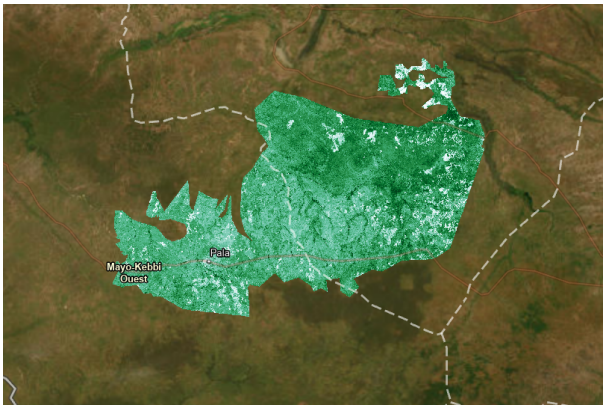
(b) Kélo



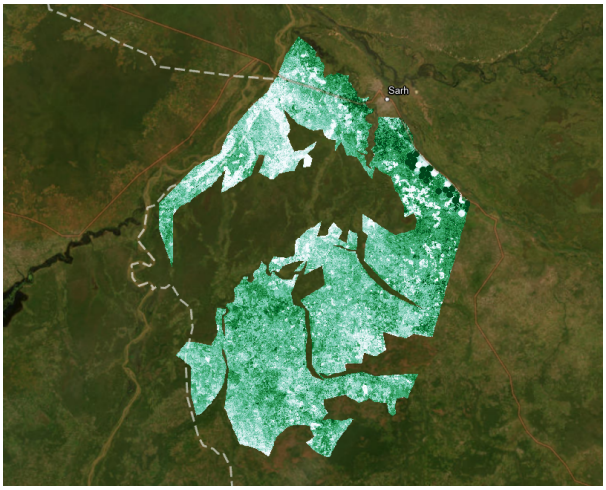
(c) Koumra



(d) Moundou

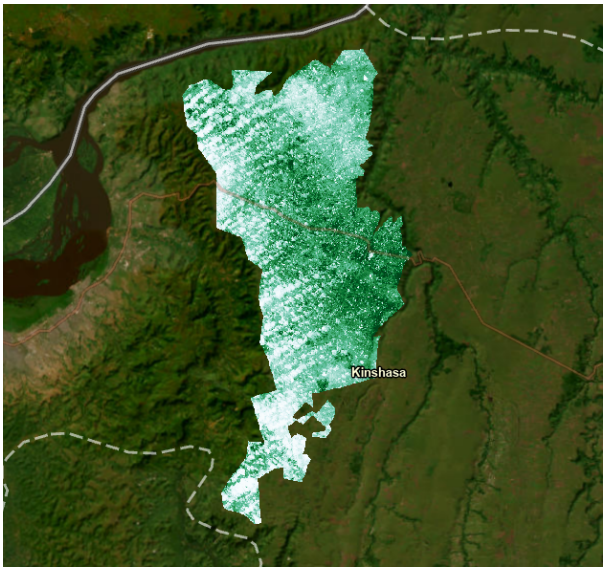


(e) Pala

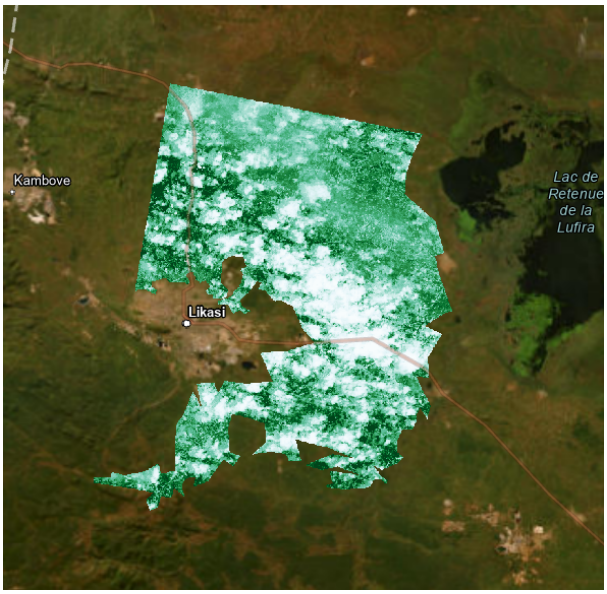


(f) Sarh

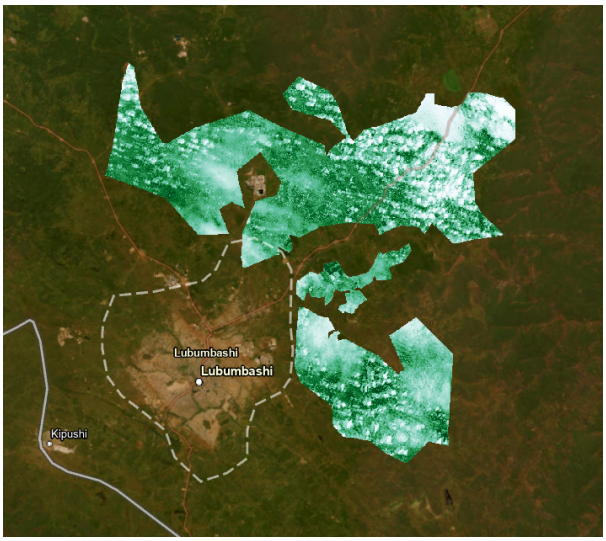
Figure A.11: Democratic Republic of Congo: Delineated Farmland Areas



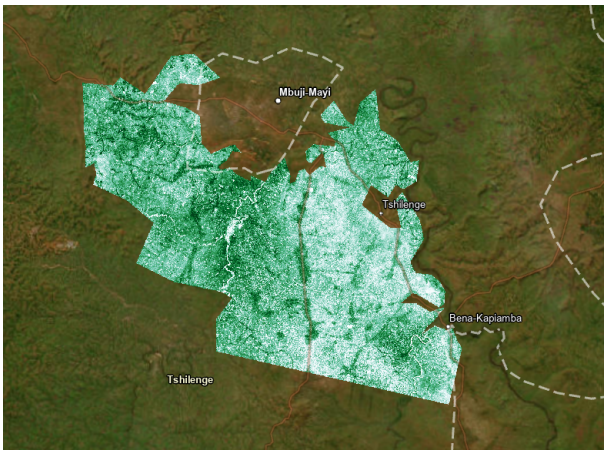
(a) Kinshasa



(b) Likasi

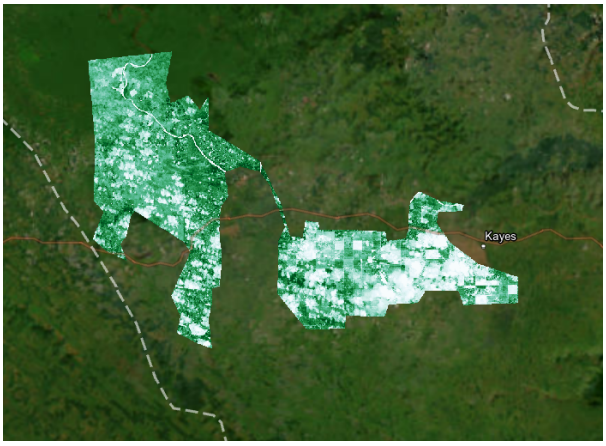


(c) Lubumbashi

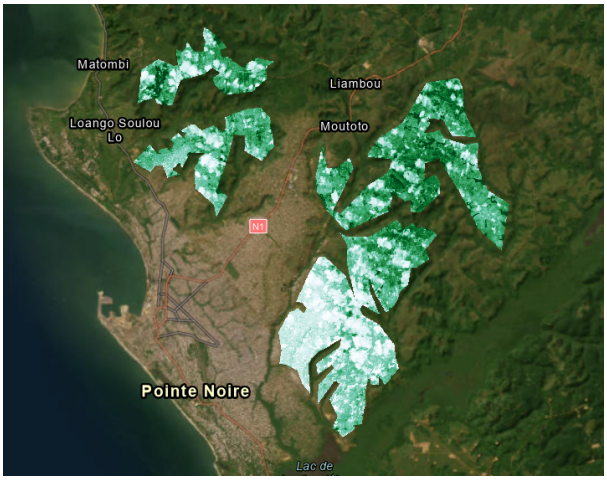


(d) Mbuji-Mayi

Figure A.12: Republic of Congo: Delineated Farmland Areas

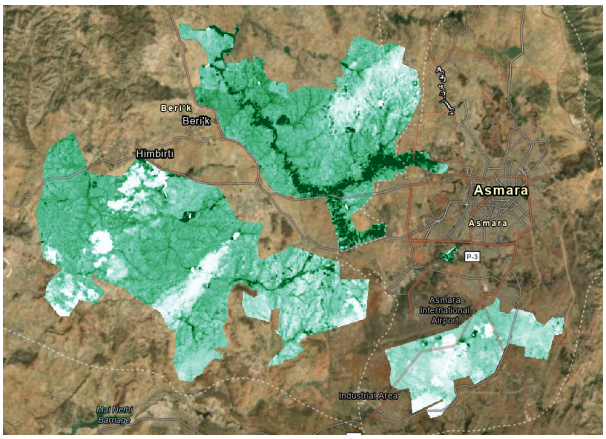


(a) Kayes

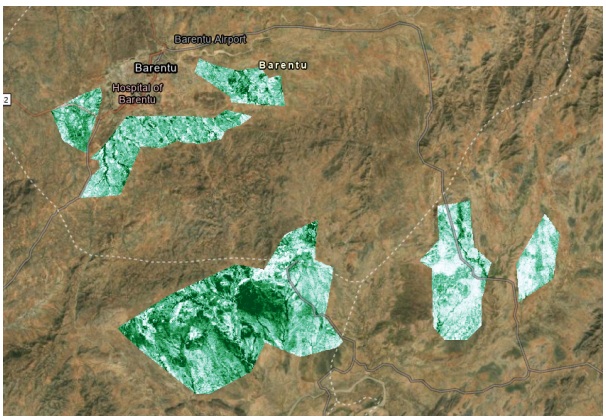


(b) Pointe-Noire

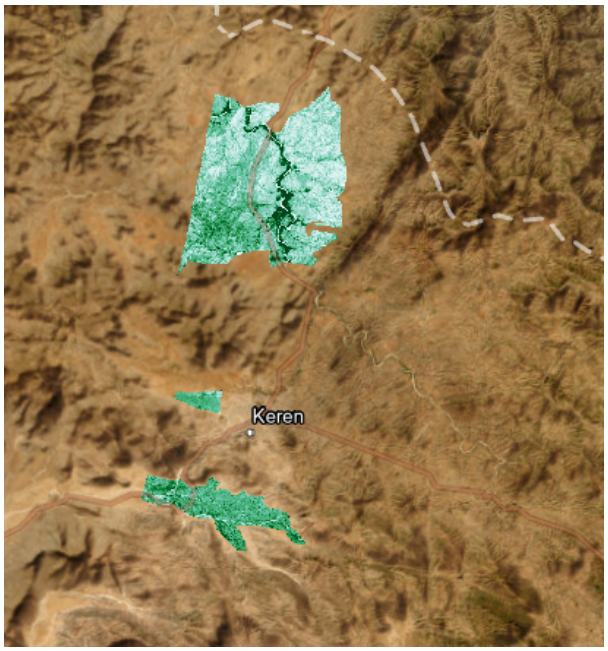
Figure A.13: Eritrea: Delineated Farmland Areas



(a) Asmara

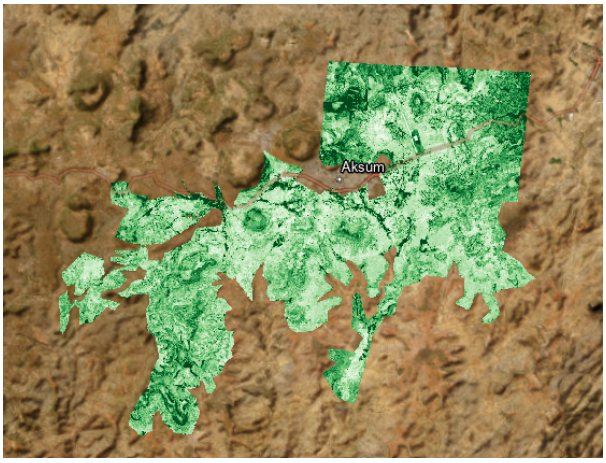


(b) Barentu

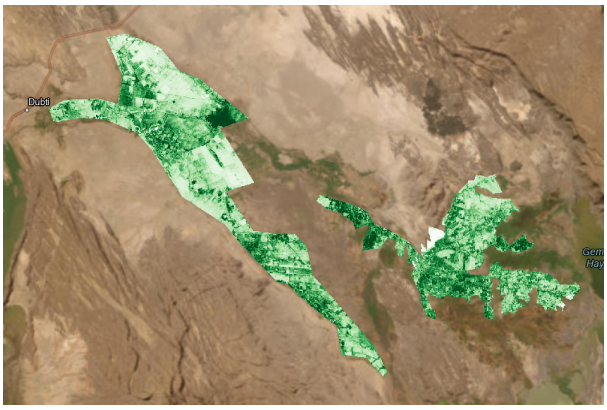


(c) Keren

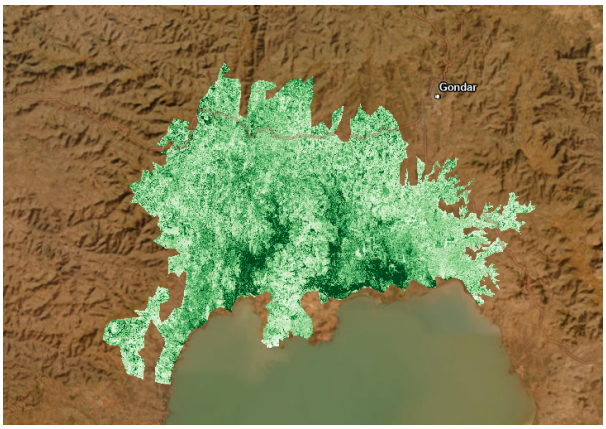
Figure A.14: Ethiopia: Delineated Farmland Areas



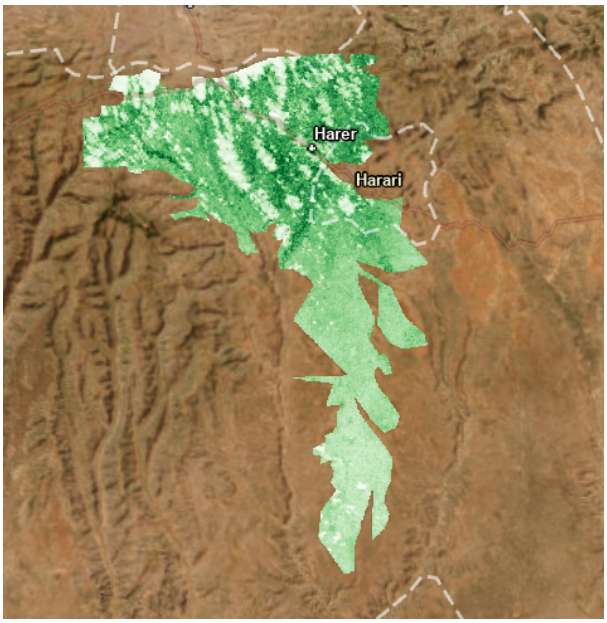
(a) Axum



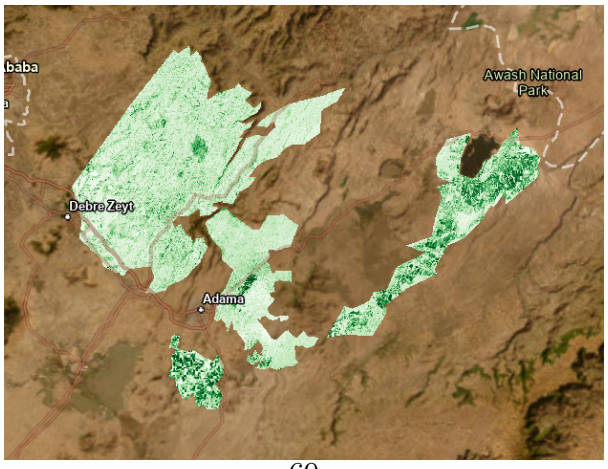
(b) Dubti



(c) Gondar

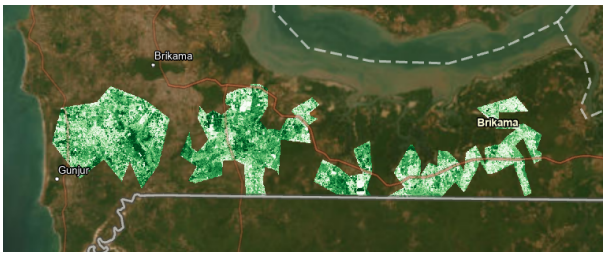


(d) Harar

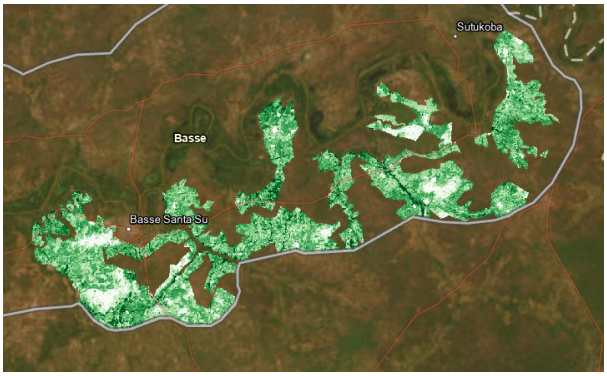


(e) Nazret / Adama

Figure A.15: Gambia: Delineated Farmland Areas



(a) Brikama

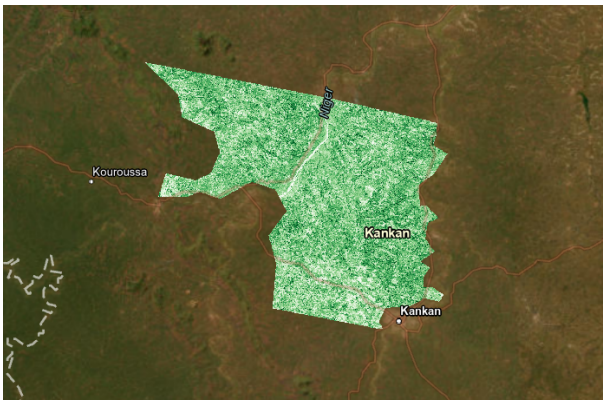


(b) Basse

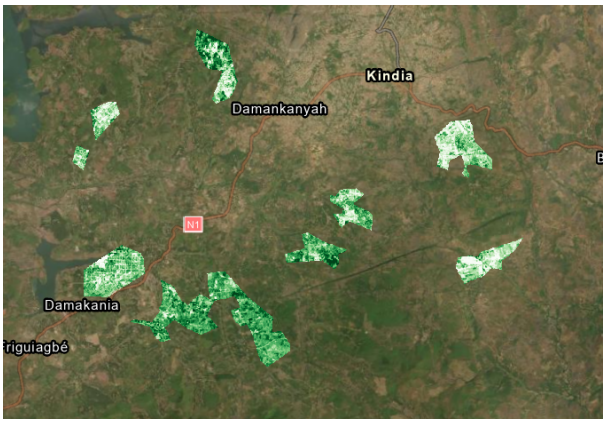


(c) Farafenni

Figure A.16: Guinea: Delineated Farmland Areas

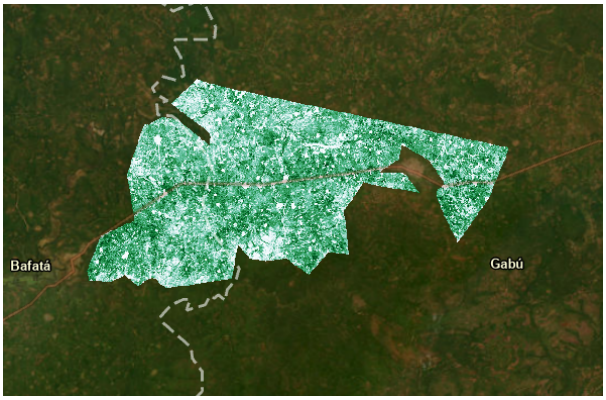


(a) Kankan

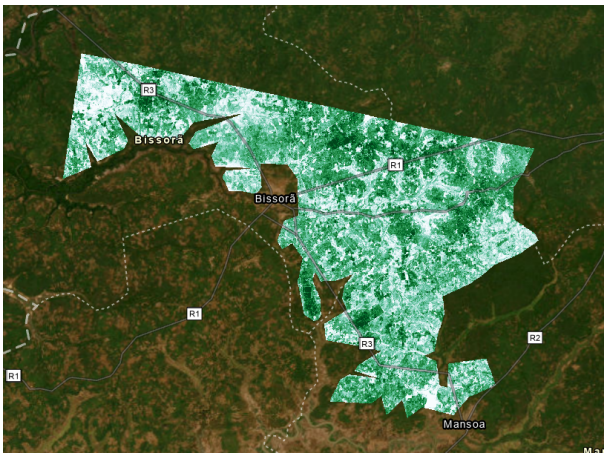


(b) Kindia

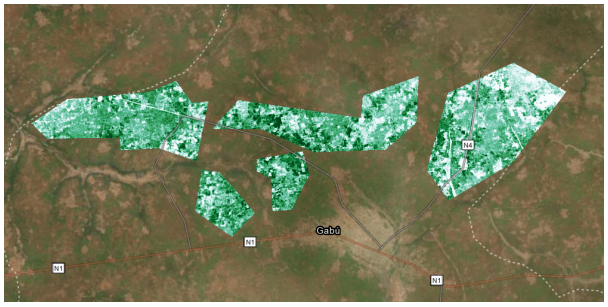
Figure A.17: Guinea-Bissau: Delineated Farmland Areas



(a) Bafatá



(b) Bissora



(c) Gabú

Note: Additional city-level satellite images for Cambodia, Georgia, Haiti, Iraq, Kosovo, Laos, Lebanon, Liberia, Libya, Mali, Mozambique, Myanmar, Nepal, Niger, Nigeria, Somalia, Sudan, Syria, Tajikistan, Togo, Uzbekistan, Venezuela, Yemen, and Zimbabwe are available in the supplementary materials.